MS#ONC-2005-02069
Oncogene
Revised March 20, 2006

7-bromoindirubin-3'-oxime induces caspase-independent cell death

Judit **RIBAS*** [1,2], Karima **BETTAYEB*** [1], Yoan **FERANDIN**[1], Marie **KNOCKAERT**[1], Xènia **GARROFÉ-OCHOA**[2], Frank **TOTZKE**[3], Christoph **SCHÄCHTELE**[3], Jan **MESTER**[4], Panagiotis **POLYCHRONOPOULOS**[5], Prokopios **MAGIATIS**[5], Alexios-Leandros **SKALTSOUNIS**[5], Jacint **BOIX**[2] and Laurent **MEIJER**** [1]

1. C.N.R.S., Cell Cycle Group & UPS2682, Station Biologique, B.P. 74, 29682 ROSCOFF cedex, Bretagne, FRANCE
2. Molecular Pharmacology Laboratory, DCMB, University of Lleida, School of Medicine, C/. Montserrat Roig 2, 25008 LLEIDA, Catalunya, SPAIN
3. ProQinase GmbH, Breisacher Str. 117, 79106 Freiburg, GERMANY
4. INSERM U 482, 184, rue du Faubourg Saint Antoine, 75571 PARIS Cedex 12, FRANCE
5. Division of Pharmacognosy and Natural Products Chemistry, Department of Pharmacy, University of Athens, Panepistimiopolis Zografou, GR-15771 ATHENS, GREECE

*** Equal contribution of the two first authors**

**** Correspondence should be addressed to** L. Meijer
(e-mail: <meijer@sb-roscoff.fr>; Tel. +33.(0)2.98.29.23.39; Fax 33.(0)2.98.29.23.42)

Running Title: Anti-tumor activity of 7-bromoindirubin-3'-oxime

Abbreviations: **AhR**, aryl hydrocarbon receptor; **ARNT**, aryl hydrocarbon receptor nuclear translocator; **BIO**, bromoindirubin-3'-oxime; **CDK**, cyclin-dependent kinase; **FCS**, fetal calf serum; FLT-3, FMS-like tyrosine kinase 3**; GSK-3**, glycogen synthase kinase-3; **IFNα**, interferon α; **IO**, indirubin-3'-oxime; **LDH**, lactate dehydrogenase; **MeBIO**, 1-methyl-bromoindirubin-3'-oxime; **MeIO**, 1-methyl-indirubin-3'-oxime; **MTS**, 3- (4,5-dimethylthiazol-2-yl)-5- (3-carboxymethoxyphenyl)-2- (4-sulfophenyl)-2*H* - tetrazolium; **RA**, retinoic acid; **ROS**, reactive oxygen species; **STS**, staurosporine; **TCDD**, 2,3,7,8-tetrachlorodibenzo-*p*-dioxin; **XRE**, xenobiotic-responsive element;

ABSTRACT

Indirubin, an isomer of indigo, is a reported inhibitor of cyclin-dependent kinases (CDKs) and glycogen synthase kinase-3 (GSK-3) as well as an agonist of the aryl hydrocarbon receptor (AhR). Indirubin is the active ingredient of a Traditional Chinese Medicinal recipe used against chronic myelocytic leukemia. Numerous indirubin analogs have been synthesized to optimize this promising kinase inhibitor scaffold. We here report on the cellular effects of 7-bromo-indirubin-3'-oxime (**7BIO**). In contrast to its 5-bromo- and 6-bromo- isomers, and to indirubin-3'-oxime, **7BIO** has only a marginal inhibitory activity towards CDKs and GSK-3. Unexpectedly, **7BIO** triggers a rapid cell death process distinct from apoptosis. **7BIO** induces the appearance of large pycnotic nuclei, without classical features of apoptosis such as chromatin condensation and nuclear fragmentation. **7BIO**-induced cell death is not accompanied by cytochrome C release neither by any measurable effector caspase activation. Furthermore, the death process is not altered either by the presence of Q-VD-OPh, a broad spectrum caspase inhibitor, or the overexpression of Bcl.-2 and Bcl-XL proteins. Neither AhR nor p53 is required during **7BIO**-induced cell death. Thus, in contrast to previously described indirubins, **7BIO** triggers the activation of non-apoptotic cell death, possibly through necroptosis or autophagy. Although their molecular targets remain to be identified, 7-substituted indirubins may constitute a new class of potential anti-tumor compounds that would retain their activity in cells refractory to apoptosis.

INTRODUCTION

In man 518+ protein kinases and 80+ protein phosphatases control the phosphorylation of enzymes and structural proteins. Phosphorylation/dephosphorylation constitutes one of the most common yet complex post-translational cellular regulatory mechanism. Abnormal phosphorylation on specific proteins is observed in essentially all pathologies and this has stimulated an extraordinary interest in small molecular weight inhibitors of kinases and phosphatases. Protein kinases now constitute the second class of targets (after G-protein coupled receptors) used in the drug screening efforts of the pharmaceutical industry (reviews in Cohen, 2002; Fischer, 2004; Weinmann and Metternich, 2005). These efforts have received considerable support from the remarkable success story of Gleevec, one of the first commercial kinase inhibitors. Currently 55 kinase inhibitors are under clinical evaluation against diseases such as cancers, inflammation, diabetes, neurodegeneration, etc...

Cyclin-dependent kinases (CDKs) play essential functions all along the cell cycle and there are multiple examples of dysfunctions of CDKs and their regulators in cancer (Vermeulen et al. 2003). Furthermore CDKs are involved in various neurodegenerative diseases such as Alzheimer's, Parkinson's and Nieman-Pick's diseases, ischemia and traumatic brain injury. A few academic groups, and most pharmaceutical companies, have thus invested in the search for pharmacological inhibitors of CDKs (reviews in Knockaert et al., 2002; Fischer et al., 2003; Benson et al., 2005; Fischer and Gianella-Borradori, 2005). Optimization of such inhibitors has been efficiently assisted by their co-crystallization with CDK2 (Noble et al., 2004), CDK5 (Mapelli et al., 2005) and CDK6 (Lu et al., 2005).

The bis-indole alkaloid indirubin and its analogs (collectively referred to as indirubins) were among some of the early CDK inhibitors to be discovered (Hoessel et al., 1999). The red/purple indirubin is an isomer of the blue indigo. Both derive from the spontaneous, non-enzymatic dimerisation of isatin and indoxyl, two precursors found either free or conjugated to carbohydrates in natural sources. Indirubins can indeed be extracted from various indigo dye producing plants (200+ species) (Balfour-Paul, 1998). They are also present in the historic "Tyrean purple" dye extracted from various

Muricidae mollusks (15+ species) (Meijer et al., 2003; review in Cooksey, 2001). They are also extracted from various wild-type and recombinant bacteria (Guengerich et al., 2004; Wu et al., 2005 and references therein). Finally, indirubin and indigo are occasionally present in human urine (Adachi et al., 2001 and references therein). Interestingly, indirubin is the active ingredient of a Traditional Chinese Medicine recipe, Danggui Longhui Wan, used to treat various diseases including chronic myelocytic leukemia (review in Xiao et al., 2002). Besides CDKs, indirubins were found to target glycogen synthase kinase -3 (GSK-3) (Leclerc et al., 2001), glycogen phosphorylase b (Kosmopoulou et al., 2004) and the aryl hydrocarbon receptor (AhR), also known as the dioxin receptor (Adachi et al., 2001; Kawanishi et al., 2003). AhR mediates the effects of many xenobiotics such as dioxin and indole-containing compounds (review in Denison & Nagy, 2003). Upon binding to xenobiotic-responsive element (XRE), activated AhR induces the transcription of numerous genes, including cytochrome P450 CYP1A1, $p27^{kip1}$, myristoyltransferase, etc... (review in Elferink, 2003). Evidence suggests that the anti-proliferative effects of indirubins derive from their ability to inhibit CDKs (Marko et al., 2001; Damiens et al., 2001). However interaction with AhR and the subsequent induction of $p27^{kip1}$ contributes to a marked arrest in G1 (Knockaert et al., 2004). Finally it has been recently shown that some indirubins prevent the phosphorylation and subsequent activation of the transcription factor STAT3, leading to a down-regulation of survival factors such as survivin and Mcl-1, and subsequent induction of cell death (Nam et al., 2005).

In this article we report on a new sub-family of indirubins, substituted on position 7. Unexpectedly, despite weak or insignificant inhibitory activity on various classical kinase targets of indirubins, 7-bromoindirubin-3'-oxime potently induces a rapid cell death distinct from classical apoptosis. The possible mechanisms of action of 7-substituted indirubins and their potential as anti-tumor agents will be discussed.

RESULTS

Different bromoindirubins display different selectivities for kinases

In a previous study we observed that a bromine substitution of indirubins on position 6 led to compounds with increased selectivity towards GSK-3 (Meijer et al., 2003; Polychronopoulos et al., 2004). We further extended this work by synthesizing and comparing indirubin-3'-oxime (**IO**) and 5-bromo- (**5BIO**), 6-bromo- (**6BIO**) or 7-bromo-indirubin-3'-oxime (**7BIO**) (Table 1). Surprisingly, compared to **IO**, **5BIO** and **6BIO, 7BIO** displayed very weak inhibitory activity towards our routine screening kinase targets, GSK-3, CDK1/cyclin B, CDK5/p25. Replacement of the bromine substituent by chlorine (**7CIO**) or iodine (**7IIO**) did not improve the potency of the 7-halogeno-indirubin-3'oximes, whereas substitution with fluorine (**7FIO**) enhanced the kinase inhibitory potency (Table 1). Finally, substitution of **7BIO** on N1 with a methyl group (**Me7BIO**) led to a completely inactive compound, as previously observed with **Me6BIO** (Meijer et al., 2003).

We next investigated the selectivity of **IO**, **5BIO**, **6BIO** and **7BIO** in the 85 kinase ProQinase selectivity panel (Table 2) [1]. This approach first revealed that Aurora A-C, FLT3, RET constitute new targets of **IO**, **5BIO** and **6BIO**. VEGF-R had been described as a target for indirubins (Jautelat et al., 2005). The selectivity panel also revealed that, compared to the three other indirubins, **7BIO** is a poor kinase inhibitor. Only one kinase, FLT3, was inhibited by **7BIO** with an IC_{50} below 1 μM (Table 2) (15 kinases for **IO**, 11 for **5BIO**, 19 for **6BIO**). 7-Br-, 7Cl- and 7I-substituted indirubin-3'-oximes showed a significant inhibitory activity towards Aurora C, a modest activity on Aurora B and little activity, if any, on Aurora A (Table 1), while **7FIO** appeared to be equipotent on the three Aurora forms. Unexpectedly **Me7BIO** was found to be rather active on Aurora C, but completely inactive on Aurora A and B (Table 1). FLT3 was found to be sensitive to all eight indirubins tested including **7MeBIO**. The effects of indirubins on Aurora kinases and FLT3 will be reported in detail elsewhere.

[1] In contrast to the above-mentioned kinase assays performed at a final 15 μM ATP concentration, the ProQinase assays are run in the absence of cold ATP. As indirubins act by competing with ATP binding the IC_{50} values are dependent on the assay ATP concnetration, therefore the values of Table 1 and 2 cannot be compared directly.

Induction of cell death by indirubins

We next compared the four indirubins for their ability to induce cell death in neuroblastoma SH-SY5Y cells as measured with an MTS reduction assay (Figure 1A). Since MTS reduction is occasionally observed under conditions different from cell death, we used an independent cell death assay, the lactate dehydrogenase (LDH) release assay (Figure 1B). Dose-response curves showed that **7BIO** is the most potent compound in terms of concentration required to reduce cell survival (MTS reduction) (Figure 1A) or in terms of cell death (LDH release) (Figure 1B). However **7BIO**'s efficacy was sensitive to the concentration of serum, suggesting that it binds to serum proteins (data not shown). Different halogens were introduced in position 7 of indirubin-3'-oxime (Figure 2, Table 1). **7FIO** was poorly active on cells compared to the equipotent **7BIO** and **7CIO**. **7IIO** was the most potent compound (Figure 2A). These results did not correlate with those obtained in the *in vitro* kinase assays (Table 1). Methylation on N1, leading to **Me7BIO**, totally abolished the cell death inducing ability of **7BIO** (Figure 2B). As **7BIO** was a poor inhibitor of kinases and yet a potent cell death inducer, we decided to investigate the effects of this compound in more detail.

To ascertain that the induction of cell death by **7BIO** was not a specific property of SH-SY5Y cells, we also used the breast cancer cell line MDA-MB-231 (Figure 3). A 48 h exposure to **7BIO** induced a dose-dependent inhibition of cell proliferation as evidenced by direct counting. This effect was poorly if at all reversible by removal of **7BIO** (Figure 3A). We next analyzed the effects of **7BIO** on cell cycle distribution (Figure 3B). A tendency towards accumulation in G2/M and reduction of G0/G1 was observed, as previously described for other indirubins (Hoessel et al., 1999; Damien et al., 2001; Marko et al., 2001).

Induction of cell death by 7BIO does not require AhR

Indirubins interact with AhR(Adachi et al., 2001). This interaction may contribute to the cellular effects of indirubins (Knockaert et al., 2004). However SH-SY5Y cells seem to be devoid of AhR (unpublished data). To evaluate the contribution of AhR to the cell death effects of **7BIO** we made use of two hepatoma cell lines, 5L (AhR +/+) and its AhR-deficient sub-clone, BP8 (AhR -/-) (Weiss et al, 1996; Kolluri et al., 1999)

(Knockaert et al., 2004). We first confirmed that, like 2,3,7,8-tetrachlorodibenzo-*p*-dioxin (TCDD) (dioxin), both **7BIO** and **Me7BIO** potently enhance the AhR -dependent expression of the CDK inhibitory protein $p27^{Kip1}$ (Figure 4A), as previously reported for **IO** and **6BIO** and their methylated counterparts, **MeIO** and **Me6BIO** (Knockaert et al., 2004). No correlation is thus observed between induction of $p27^{Kip1}$ expression (Figure 4A) and induction of cell death (Figure 2B). We next analyzed the effects of **7BIO** and **Me7BIO** on cell cycle distribution of AhR-/- and AhR+/+ cells. As reported for other indirubins, both **7BIO** and **Me7BIO** induced a striking AhR-dependent accumulation in G0/G1 (Figure 4B). Finally cell death induction was estimated in both cell lines following exposure to increased **7BIO** concentrations. The dose-response curves were essentially the same (Figure 4C). Altogether these results show that AhR is not involved in the cell death inducing properties of **7BIO**.

7BIO-induced cell death involves neither p53 nor $p21^{Cip1}$ nor STAT3 dephosphorylation

We next investigated the involvement of p53 and $p21^{Cip1}$ in cell death induced by the four indirubins (Figure 5). P53 was strongly induced by **5BIO** in a time-dependent manner in SH-SY5Y cells (Figure 5A-B). Induction of p53 was only modest in cells treated with **6BIO** and insignificant in cells treated with **IO**, **7BIO** or **Me7BIO** (Figure 5A-B). As expected, analysis of $p21^{Cip1}$ expression under the same conditions showed a time-dependent induction by **5BIO** (Figure 5C). $p21^{Cip1}$ expression occurred with some delay after p53 stabilization (Figure 5B). **IO**, **5BIO** and **6BIO** were roughly equipotent at inducing $p21^{Cip1}$overexpression, while **7BIO** and **Me7BIO** had negligible effects (Figure 5A). Finally, we tested the effects of **7BIO** on wild-type HCT-116 and HCT-116 sub-clones deprived of p53 (Figure 5E). The dose-response curves were essentially the same. Altogether these data suggest that **7BIO**-induced cell death does not induce p53 nor require its contribution.

Tyrosine phosphorylation and subsequent activation of the transcription factor STAT3 were recently shown to be inhibited by some indirubins, leading to the down-regulation of survival factors and subsequent induction of cell death (Nam et al., 2005). To examine whether this mechanism is involved in the action of **7BIO**, we investigated

the effect from **IO**, **5BIO**, **6BIO** and **7BIO** on the level of tyrosine 705-phosphorylated STAT3 in MDA-MB-231 cells (Figure 6). As a positive control, cells were also stimulated by interferon α (IFNα). Results show that the basal level of tyrosine 705-phosphorylated STAT3 in MDA-MB-231 is very low compared to the level reached by stimulation with IFNα, yet it is down-regulated by **IO**, **5BIO** and **6BIO** but not by **7BIO**. This suggests that the mechanism of action of **7BIO** is not primarily due to an inactivation of tyrosine phosphorylated STAT3.

Induction of cell death by 7BIO is much faster than by other indirubins

A time-course of SH-SY5Y cell death induction was next performed following exposure to 25 μM **IO**, **5BIO**, **6BIO**, **7BIO** or **Me7BIO** (Figure 7). Although **5BIO** and **6BIO** required 36-48 h to induce 70 % cell death, this level was reached by 12 h with **7BIO**. Almost complete cell death was obtained with **7BIO** within 24 h (Figure 7). This much faster kinetics suggests that a different mechanism of cell death is occurring in the case of **7BIO** compared to the other indirubins. Alternatively a sub-population of cells may respond to **5BIO** and **6BIO** as they do to **7BIO**, while the vast majority undergoes apoptosis.

7BIO induces non-apoptotic cell death

To investigate the mechanism of action of **7BIO** we first examined, under a fluorescence microscope, SH-SY5Y cells exposed to different indirubins following bisBenzimide and propidium iodide (PI) staining (Figure 8). First of all, no PI staining was observed in control cells and in **Me7BIO**-treated cells (Figure 8A, 8F), confirming the absence of cell death. **IO**, **5BIO** and **6BIO** all triggered nuclear fragmentation typical of apoptosis, accompanied by secondary necrosis (Figure 8B-8D). These figures were never observed in **7BIO**-treated cells which, in contrast, displayed numerous large, unfragmented pycnotic nuclei (Figure 8E). Such figures were observed only occasionally with **5BIO** and **6BIO** (Figure 8C-8D). These morphological results suggest that **7BIO** triggers an atypical cell death different from apoptosis.

To challenge this possibility, the activity of caspases was assayed in SH-SY5Y cells exposed to various concentrations of different indirubins (Figure 9). **5BIO** and

6BIO, and **IO** to a lesser extent, triggered a dose- (Figure 9A) and time- (Figure 9B) dependent activation of caspase activity. In sharp contrast, neither **7BIO** nor **Me7BIO** induced any activation of caspases which remained at the level of control, untreated cells. Furthermore, Q-VD-Oph, a general caspase inhibitor (Caserta et al., 2003), had no effect on cell death induced by **7BIO** (Figure 10), while it reduced the level of cell death induced by **5BIO** and **6BIO**, and **IO**, to a lesser extent (Figure 10A). The time-course of **7BIO**-induced cell death was unaffected by Q-VD-Oph (Figure 10B).

Moreover, **7BIO** triggered negligible release of cytochrome C from mitochondria (Figure 11). Under the same conditions **IO**, **5BIO** and **6BIO** induced the release of cytochrome C to levels similar to those reached by standard apoptosis-inducing reagents like staurosporine and etoposide. We next examined DNA laddering as a reflection of apoptotic cell death. The laddering caused by R-Roscovitine was consistent with the reported ability of this compound to induce apoptosis (Ribas and Boix, 2004). **5BIO** and to a lesser extent **6BIO,** also induced internuclesosomal fragmentation, which intensity was proportional to the amount of apoptotic cells in the culture (see bisBenzimide/propidium iodide staining in Figure 8). In **7BIO** treated cells no ladder was observed, however most cells were dead. In **Me7BIO**, **IO** and **DMSO** treatments, cell death induction was negligible and no laddering was detected.

Altogether these results show that **7BIO**-induced cell death does not induce cytochrome C release and does not trigger nor require the activation of caspases, in sharp contrast with cell death induced by **IO**, **5BIO** and **6BIO**. Thus **7BIO** appears to induce a cell death pathway which differs from the apoptosis induced by **IO**, **5BIO** and **6BIO**.

7BIO-induced cell death is not inhibited by cellular mechanisms able to protect cells from apoptosis.

To further explore the cell death process triggered by **7BIO**, we wondered if proved mechanisms of resistance to apoptosis were able to protect cells from **7BIO**'s effects. SH-SY5Y cells can be differentiated in cell culture by retinoic acid (RA) and this differentiation prevents apoptosis triggered by CDK inhibitors, like olomoucine or roscovitine (Ribas and Boix, 2004). Similarly, differentiation renders SH-SY5Y cells refractory to staurosporine (STS), an established agent used to induce canonical

apoptosis. As shown in Figure 12, differentiation had negligible effect on the rates of **7BIO**-induced cell death.

Bcl-2 and Bcl-XL proteins are known for their anti-apoptotic effects. In addition, their cytoprotective effects have been found to extend beyond apoptosis (Kane et al, 1995). We previously described that Bcl-2 and Bcl-XL overexpression protects SH-SY5Y cells from apoptosis triggered by STS (Yuste et al., 2002). As reported, Bcl-XL surpassed Bcl-2 at inhibiting STS-induced apoptosis (Figure 12B). However, in a parallel time course experiment, neither Bcl-XL nor Bcl-2 overexpression provided any significant protection from **7BIO** (Figure 12B). Taken together, these results reinforce the action of **7BIO** as an effective cell killer acting in an apoptosis independent manner.

Non-apoptotic, caspase-independent cell death is a general characteristic of the death processes triggered by 7BIO

To challenge the generality of the **7BIO** effects, we tested **7BIO** in two other human neuroblastoma derived cell lines, IMR-5 and IMR-32, as well as two hematological tumors derived cell lines, Jurkat and HL-60. As shown in Figure 13 (left column), **7BIO** induced cell death in the same range of concentrations characterized as lethal for SH-SY5Y, MDA-MB-231 (breast cancer) and HCT116 (colon cancer) cell types. The sensitivity of HL-60 cells (known to be deficient in p53 protein) to **7BIO** is consistent with the lack of involvement of p53 as described above.

We further characterized the cell death process triggered by **7BIO** in IMR-5, IMR-32, Jurkat and HL-60 cells. Bis-benzimide staining, fluorescence and electron microcopy characterizations demonstrated that non-apoptotic cell death was taking place as described in SH-SY5Y cells (data not shown). In addition, effector caspase activation was assessed at 24 h (Figure 13, right). As expected, **5BIO** triggered caspase activation. Compared with STS, **5BIO** displayed reduced caspase activation, consistent with (1) the mixed type of cell death **5BIO** induces and (2) less synchronous kinetics of apoptosis induction. In contrast DEVDase activity in **7BIO**-treated cells fell consistently below the background displayed by control, untreated cells. In conclusion, the non-apoptotic, caspase-independent type of cell death triggered by **7BIO** appears to be an intrinsic property of the compound, independent of cell model.

DISCUSSION

Indirubins have been the object of many chemical modulations in order to improve their selectivity profile, kinase inhibitory efficacy and solubility. In particular numerous modifications have been carried out on positions 3', 5', 6' on one indole ring and 5 or 6 on the other indole ring (Hoessel et al., 1999; Leclerc et al., 2000; Meijer et al., 2003; Merz et al., 2004; Polychronopoulos et al., 2004; Jautelat et al., 2005). However no modifications have ever been reported on position 7. One reason might be that substitution at this position almost annihilates inhibitory activity towards key targets of indirubins, CDKs and GSK-3. The fast and potent induction of cell death by **7BIO** was totally unexpected, but provided the impetus to investigate 7-substituted indirubins further. Indirubins have been co-crystallized with CDK2 (Hoessel et al., 1999), CDK2/cyclin A (Davies et al., 2001), CDK5 (Mapelli et al., 2005), PfPK5, the *Plasmodium falciparum* homolog of CDK1 (Holton et al., 2004), GSK-3ß (Bertrand et al., 2003; Meijer et al., 2003; Polychronopoulos et al., 2004), and glycogen phosphorylase b (Kosmopoulou et al., 2004). These co-crystal structures suggest that a bromine substitution on position 7 would be detrimental to the interaction of indirubins with their targets as will be described in detail elsewhere (in preparation). A general steric hindrance by the bromine is supported by the fact that **IO** substituted with a small atom such as fluorine is much more active toward kinases than when the position 7 is substituted with other halogens (Table 1). This overall unfavorable position 7 substitution is confirmed by the kinase selectivity panel (Table 2) which shows that, compared to **IO**, **5BIO** and **6BIO**, **7BIO** interacts poorly with protein kinases. However this panel only represents 85 out of 518 kinases and the possibility that **7BIO** potently inhibits one or several unidentified kinases remains open. In addition **7BIO** may bind to its targets in an orientation which is widely different from that of **IO** and **6BIO** in CDKs and GSK-3.

Indirubins appear to induce different forms of cell death according to their substitutions. We previously reported that a transient exposure to **IO** triggered a necrotic type cell death in nocodazole-synchronized HBL100 cells (Damiens et al., 2001). In contrast **IO** apparently triggered apoptotic type cell death in MCF-7 cells (Marko et al., 2001). Various 5-substituted indirubins also induce apoptosis as evidenced by PARP

cleavage (Nam et al., 2005). This apoptosis appears to be correlated with down-regulation of survival factors such as survivin and Mcl-1. Induction of apoptosis has also been recently described for 5-nitro-indirubin-3'-oxime (Lee et al., 2005).

Six arguments demonstrate that **7BIO** induces cell death by a mechanism distinct from apoptosis: [1] a morphological study of dying cells shows that **7BIO** induces the appearance of large pycnotic nuclei, without classical features of apoptosis such as nuclear fragmentation and secondary necrosis (Figure 8); [2] **7BIO** does not trigger an activation of caspases (Figure 9, 13); [3] the general caspase inhibitor Q-VD-OPh does not counteract **7BIO**-induced cell death (Figure 10); [4] **7BIO** does not induce cytochrome C release (Figure 11); [5] **7BIO** does not induce DNA fragmentation (Figure 9); [6] neither Bcl-2 nor Bc-XL overexpression significantly reduce the level of **7BIO**-induced cell death (Figure 12B).

What is the nature of **7BIO**-induced cell death ? Besides apoptosis, a number of caspase-independent cell death mechanisms have been described (reviews in Jäättelä, 2004; Broker et al, 2005). One such pathway is autophagy, a cellular process involved both in cell survival and in cell death which requires the family of Atg genes (review in Baehecke, 2005). Whether such a pathway is involved in **7BIO**-induced cell death is currently under investigation. Recently a new caspase-independent cell death process, necroptosis, was described that displays some of the characteristics of necrosis and activation of autophagy (Degterev et al., 2005). We are currently investigating this pathway as a potential mechanism of action of **7BIO**. Interestingly it is inhibited by a family of substituted indoles called necrostatins (Degterev et al., 2005). Substituents (methyl, halogen) at position 7 on necrostatin result in increased inhibitory activity (Teng et al., 2005). Given their partial structure similarity it is tempting to speculate that necrostatins and **7BIO** might share a target which they affect in opposite directions. Another description of caspase-independent cell death implies the generation of reactive oxygen species (ROS) (Chipuk and Green, 2005). Although preliminary experiments suggest that **7BIO** does not induce the generation of ROS in vitro (unpublished), we are still exploring this possible mechanism of action of **7BIO**. Electron microscopy examination of **7BIO**-treated cells reveals that **7BIO** induces a prominent disruption of

endoplasmic reticulum without markedly affecting the nucleus (data not shown), suggesting that **7BIO** acts as a potent reticulum stress inducer.

Indirubins interact with and activate AhR leading to the up-regulation of cytochrome P450 and $p27^{Kip1}$ (Adachi et al., 2001; Spink et al., 2003; Knockaert et al., 2004; Sugihara et al., 2004). **7BIO** clearly activates AhR as observed in an in vitro luciferase reporter system (unpublished), and confirmed by the AhR-dependent expression of $p27^{Kip1}$ and G1 arrest (Figure 4). However three pieces of evidence suggest that AhR is not involved in the cell death process induced by **7BIO**: [1] **7BIO** triggers cell death equally well in AhR-/- and AhR+/+ cells; [2] neuroblastoma SH-SY5Y cells express very little if any AhR (unpublished); [3] **MeBIO**, which is as potent as **7BIO** in activating AhR, does not induce cell death.

7BIO inhibits Aurora C and FLT-3 (Table 1 and unpublished data). Yet **Me7BIO**, which is as potent as **7BIO** at inhibiting both kinases, does not trigger cell death (Figure 2B). **7BIO**-induced cell death is therefore unlikely to be a direct consequence of inhibition of these two kinases. We also believe that **7BIO** action does not involve the down-regulation of STAT3 tyrosine phosphorylation and its subsequent inactivation as has been suggested for other indirubins (Nam et al., 2005) (Figure 11).

Although it is too early to speculate on the potential clinical use of 7-substituted indirubins, this new family of indirubins opens a promising research area. Firstly, these molecules seem to interact with much less kinases than previously described indirubins and thus appear to be more selective (Table 2). Identification of the molecular targets of **7BIO** and 7-substituted indirubins obviously constitutes a high priority. We plan to tackle this using affinity chomatography on immobilized **7BIO** as described for other kinase inhibitors (Bach et al., 2006). Secondly, numerous cancer cells are characterized by the development of various mechanisms of resistance to apoptosis (for instance overexpression of the Bcl-2 and Bcl-XL oncogenic proteins). Such tumor cells thus constitute putative targets for 7-substituted indirubins such as **7BIO**, which induce cell death through a non-apoptotic pathway and in a Bcl2/Bcl-XL-insensitive way. Such indirubins might thus allow the killing of tumor cells resistant to conventional anticancer drugs.

MATERIAL & METHODS

Chemistry

General chemistry experimental procedures

All chemicals were purchased from Aldrich Chemical Co. NMR spectra were recorded on Bruker DRX 400; chemical shifts are expressed in ppm downfield from TMS. The ^{1}H-^{1}H and the ^{1}H-^{13}C NMR experiments were performed using standard Bruker microprograms. CI-MS spectra were determined on a Finnigan GCQ *Plus* ion-trap mass spectrometer using CH_4 as the CI ionization reagent. Column chomatographies were conducted using flash silica gel 60 Merck (40-63 μm), with an overpressure of 300 mbars. All the compounds gave satisfactory combustion analyses (C, H, N, within ± 0.4% of calculated values).

Indirubin synthesis general procedures

5-Bromoindirubin (**5BI**), 7-bromoindirubin (**7BI**), 7-chloroindirubin (**7CI**), 7-iodoindirubin (**7II**), 7-fluoroindirubin (**7FI**) and 7-bromo-1-methylindirubin (**Me7BI**) were prepared from 5-bromoisatin, 7-bromoisatin, 7-chloroisatin, 7-iodoisatin, 7-fluoroisatin, 7-bromo-1-methylisatin, respectively, and 3-acetoxyindol. The synthesis of the corresponding indirubins and isatins will be described in details elsewhere (Polychronopoulos et al, in preparation)

5-Bromoindirubin-3'-oxime (**5BIO**), 7-bromoindirubin-3'-oxime (**7BIO**), 7-chloroindirubin-3'-oxime (**7CIO**), 7-iodoindirubin-3'-oxime (**7IIO**) 7-fluoroindirubin-3'-oxime (**7FIO**) and 1-methyl-7-bromoindirubin-3'-oxime (**Me7BIO**) were prepared from the corresponding indirubins and hydroxylamine hydrochloride. **IO** and **6BIO** were synthesized as previously described (Leclerc et al, 2001; Polychronopoulos et al, 2004).

General procedure for the preparation of the indirubin-oximes 5BIO, 7BIO, 7CIO, 7IIO, 7FIO and Me7BIO

The appropriate indirubin derivative **5BI**, **7BI**, **7CI**, **7II**, **7FI** or **Me7BI** (1 mmol) was dissolved in pyridine (10 mL). With magnetic stirring, hydroxylamine hydrochloride (10 equiv) was added and the mixture was heated under reflux (120 ^{o}C) for 1.5 h. Then the solvent was evaporated under reduced pressure and the residue was washed with water and cyclohexane to afford quantitatively the corresponding 3'-oxime.

5-Bromoindirubin-3'-oxime (5BIO)

^{1}H NMR (DMSO, 400 MHz, δ ppm, *J* σε Hz) 13.70 (1H, s, NOH), 11.83 (1H, s, N'-H), 10.87 (1H, s, N-H), 8.76 (1H, d, *J* = 2.1 Hz, H-4), 8.27 (1H, d, *J* = 7.9 Hz, H-4'), 7.44 (2H, m, H-6', 7'), 7.28 (1H, dd, *J* = 8.2, 2.0 Hz, H-6), 7.06 (1H, td, *J* = 7.9, 2.0 Hz, H-5'), 6.85 (1H, d, *J* = 8.2 Hz, H-7); CI-MS *m/z* 356, 358 $(M+H)^+$

7-Bromoindirubin-3'-oxime (7BIO)

^{1}H NMR (DMSO, 400 MHz, δ ppm, *J* σε Hz) 13.68 (1H, brs, NOH) 11.90 (1H, s, N'-H), 10.91 (1H, s, N-H), 8.67 (1H, d, *J* = 7.8 Hz, H-4), 8.23 (1H, d, *J* = 7.8, H-4'), 7.42 (2H, m, H-6', 7'), 7.29 (1H, d, *J* = 7.8 Hz, H-6), 7.06 (1H, t, *J* = 7.8 Hz, H-5'), 6.90 (1H, t, *J* = 7.8 Hz, H-5); CI-MS *m/z* 356, 358 $(M+H)^+$

7-Chloroindirubin-3'-oxime (7CIO)

^{1}H NMR (DMSO, 400 MHz, δ ppm, *J* σε Hz) 13.70 (1H, brs, NOH) 11.86 (1H, s, N'-H), 11.09 (1H, s, N-H), 8.62 (1H, d, *J* = 7.9 Hz, H-4), 8.23 (1H, d, *J* = 7.6, H-4'), 7.44 (2H, m, H-6', 7'), 7.17 (1H, d, *J* = 7.9 Hz, H-6), 7.06 (1H, t, *J* = 7.6 Hz, H-5'), 6.96 (1H, t, *J* = 7.8 Hz, H- 5); CI-MS *m/z* 312, 314 $(M+H)^+$

7-Iodoindirubin-3'-oxime (7IIO)

^{1}H NMR (DMSO, 400 MHz, δ ppm, *J* in Hz) 13.65 (1H, brs, NOH) 11.87 (1H, s, N'-H), 10.63 (1H, s, N-H), 8.68 (1H, d, *J* = 7.8 Hz, H-4), 8.23 (1H, d, *J* = 7.2, H-4'), 7.47 (1H, d, *J* = 7.8 Hz, H-6), 7.43 (2H, m, H-6', 7'), 7.06 (1H, t, *J* = 7.2 Hz, H-5'), 6.76 (1H, t, *J* = 7.8 Hz, H- 5); CI-MS *m/z* 404 $(M+H)^+$

7-Fluoroindirubin-3'-oxime (7FIO)

^{1}H NMR (DMSO, 400 MHz, δ ppm, *J* σε Hz) 13.61 (1H, brs, NOH) 11.85 (1H, s, N'-H), 11.19 (1H, s, N-H), 8.44 (1H, d, *J* = 7.8 Hz, H-4), 8.19 (1H, d, *J* = 7.5, H-4'), 7.39 (2H, m, H-6', 7'), 7.00 (2H, m, H-5', 6), 6.90 (1H, m, H-5); CI-MS *m/z* 296 $(M+H)^+$

1-Methyl-7-bromoindirubin-3'-oxime (Me7BIO)

^{1}H NMR (DMSO, 400 MHz, δ ppm, *J* σε Hz) 13.70 (1H, brs, NOH), 12.00 (1H, s, N'-H), 8.81 (1H, d, *J* = 7.9 Hz, H-4), 8.23 (1H, d, *J* = 7.9 Hz, H-4'), 7.43 (2H, m, H-6', 7'), 7.34 (1H, d, *J* = 7.9 Hz, H-6), 7.07 (1H, t, *J* = 7.9 Hz, H-5'), 6.93 (1H, t, *J* = 7.9 Hz, H-5), 3.68 (3H, s, N-CH_3); CI-MS *m/z* 370, 372 $(M+H)^+$

Protein kinase assays

Biochemical Reagents

Sodium ortho-vanadate, EGTA, EDTA, Mops, ß-glycerophosphate, phenylphosphate, sodium fluoride, dithiothreitol (DTT), glutathione-agarose, glutathione, bovine serum albumin (BSA), nitrophenylphosphate, leupeptin, aprotinin, pepstatin, soybean trypsin inhibitor, benzamidine, histone H1 (type III-S) were obtained from Sigma Chemicals. [γ-^{33}P]-ATP was obtained from Amersham. The GS-1 peptide (YRRAAVPPSPSLSRHSSPHQSpEDEEE) was synthesized by the Peptide Synthesis Unit, Institute of Biomolecular Sciences, University of Southampton, Southampton SO16 7PX, U.K.

Buffers

Homogenization Buffer: 60 mM ß-glycerophosphate, 15 mM p-nitrophenylphosphate, 25 mM Mops (pH 7.2), 15 mM EGTA, 15 mM $MgCl_2$, 1 mM DTT, 1 mM sodium vanadate, 1 mM NaF, 1 mM phenylphosphate, 10 µg leupeptin/ml, 10 µg aprotinin/ml, 10 µg soybean trypsin inhibitor/ml and 100 µM benzamidine.

Buffer A: 10 mM $MgCl_2$, 1 mM EGTA, 1 mM DTT, 25 mM Tris-HCl pH 7.5, 50 µg heparin/ml.

Buffer C: homogenization buffer but 5 mM EGTA, no NaF and no protease inhibitors.

Kinase preparations and assays

Kinase activities were assayed in Buffer A or C, at 30 °C, at a final ATP concentration of 15 µM. Blank values were subtracted and activities calculated as pmoles of phosphate incorporated for a 10 min. incubation. The activities are usually expressed in % of the maximal activity, i.e. in the absence of inhibitors. Controls were performed with appropriate dilutions of dimethylsulfoxide.

CDK1/cyclin B was extracted in homogenization buffer from M phase starfish (*Marthasterias glacialis*) oocytes and purified by affinity chromatography on $p9^{CKShs1}$-sepharose beads, from which it was eluted by free $p9^{CKShs1}$ as previously described (Meijer et al., 1997). The kinase activity was assayed in buffer C, with 1 mg histone H1 /ml, in the presence of 15 µM [γ-^{33}P] ATP (3,000 Ci/mmol; 10 mCi/ml) in a final volume of 30 µl. After 30 min. incubation at 30°C, 25 µl aliquots of supernatant were spotted onto 2.5 x 3 cm pieces of Whatman P81 phosphocellulose paper, and, 20 sec. later, the

filters were washed five times (for at least 5 min. each time) in a solution of 10 ml phosphoric acid/liter of water. The wet filters were counted in the presence of 1 ml ACS (Amersham) scintillation fluid.

CDK5/p25 was reconstituted by mixing equal amounts of recombinant mammalian CDK5 and p25 expressed in *E. coli* as GST (glutathione-S-transferase) fusion proteins and purified by affinity chomatography on glutathione-agarose (vectors kindly provided by Dr. J.H. Wang) (p25 is a truncated version of p35, the 35 kDa CDK5 activator). Its activity was assayed with histone H1 in buffer C as described for CDK1/cyclin B.

GSK-3α/β was purified from porcine brain by affinity chomatography on immobilized axin (Meijer et al., 2003). It was assayed, following a 1/100 dilution in 1 mg BSA/ml 10 mM DTT, with 5 µl 4 µM GS-1 peptide substrate, in buffer A, in the presence of 15 µM [γ-^{33}P] ATP (3,000 Ci/mmol; 10 mCi/ml) in a final volume of 30 µl. After 30 min. incubation at 30°C, 25 µl aliquots of supernatant were processed as described above.

ProQinase protein kinase assays. All protein kinases were expressed in Sf9 insect cells as human recombinant GST-fusion proteins or His-tagged proteins by means of the baculovirus expression system. Kinases were purified by affinity chomatography using either GSH-agarose (Sigma) or Ni-NTH-agarose (Qiagen). The purity and identity of each kinase was checked by SDS-PAGE/Coomassie staining and by Western blot analysis. A proprietary protein kinase assay (^{33}PanQinase® Activity Assay) was used to assay the recombinant enzymes. All kinase assays were performed in 96-well FlashPlates™ from Perkin Elmer/NEN (Boston, MA, USA) in a 50 µl reaction volume using a BeckmanCoulter/Sagian robotic system. The reaction cocktail was pipetted in four steps in the following order: (i) 20 µl of assay buffer, (ii) 5 µl of ATP solution (in H_2O), (iii) 5 µl of test compound (in 10 % DMSO) and (iv) 10 µl of substrate / 10 µl of enzyme solution (premixed). The assays for all kinases (except for PKC, see below) contained 60 mM HEPES-NaOH, pH 7.5, 3 mM $MgCl_2$, 3 mM $MnCl_2$, 3 µM Na-orthovanadate, 1.2 mM DTT, 50 µg/ml PEG_{20000}, 1 µM [γ-^{33}P]-ATP (approx. 5 x 10^5 cpm per well). The final DMSO concentration was 1% in all assays. PKC assays contained 60 mM HEPES-NaOH, pH 7.5, 1 mM EDTA, 1.25 mM EGTA, 5 mM $MgCl_2$, 1.32 mM $CaCl_2$, 5 µg/ml phosphatidylserine, 1 µg/ml 1.2 dioleyl-glycerol, 1.2 mM DTT, 50 µg/ml PEG_{20000}, 1 µM [γ -^{33}P]-ATP (approx. 5 x10^{05} cpm per well). The reaction

cocktails were incubated at 30 °C for 80 minutes. The reaction was stopped with 50 µl of 2 % (v/v) H_3PO_4, plates were aspirated and washed two times with 200 µl H_2O or 200 µl 0.9 % (w/v) NaCl. Incorporation of $^{33}P_i$ was determined with a microplate scintillation counter (Microbeta, Wallac). With the residual activities (in %) obtained for each concentration the compound IC_{50} values were calculated using Prism 3.03 for Windows (Graphpad, San Diego, CA, USA). The model used was "sigmoidal response (variable slope)" with parameters "top" fixed at 100 % and "bottom" at 0 %.

Cell biology

Chemicals and Antibodies

BisBenzimide (Hoechst 33342) and propidium iodide were obtained from Sigma Chemicals. AcDEVDafc and Q-VD-OPh was purchased from MPbiomedicals (Vannes, France). Cell Titer 96® kit containing the MTS reagent was purchased from Promega (Madison, WI, USA). 2,3,7,8-tetrachlorodibenzo-*p*-dioxin (TCDD) was a kind gift from Dr. Steve Safe (Veterinary Physiology and Pharmacology, Texas A&M University, College Station, TX77843, USA). The protease inhibitor cocktail was from Roche. IFN-α was obtained from R and D systems and *all-trans*-Retinoic Acid (RA), from Tocris (Bristol, UK). Unless otherwise stated, the non-listed reagents were also from Sigma.

Monoclonal antibodies against p21 $^{WAF1/CIP1}$ and actin were obtained from Oncogene. Antibodies against p27 ^{KIP1} and p53 were purchased from Santa Cruz Biotechnology. Monoclonal antibody against cytochrome C and rabbit polyclonal against Bcl-XL were provided by BD Biosciences. AntiBcl-2 (clone 124) monoclonal antibody was purchased from DAKO. Anti-PhosphoTyr705-STAT3 and anti-STAT3 antibodies were from Cell Signalling. The anti-tubulin antibody was from Sigma.

Cell lines and culture conditions

The mouse 5L hepatoma cell line (AhR +/+) and BP8 (an AhR -/- subclone) were kindly provided by Dr. M. Goëttlicher (Forschungszentrum Karlsruhe, Institute of Genetics, 76021 Karlsruhe, Germany). They were cultured in Dulbecco's modified Eagle medium (DMEM) (Biowhittaker) supplemented with 2 mM L-glutamine (Eurobio), 10 % fetal calf serum (FCS), and gentamycin (Gibco BRL) at 37°C in an atmosphere of 7 % CO_2. Indirubin or TCDD treatments were performed on 50-60 % confluent cultures at the

indicated time and concentrations. Control experiments were carried out using appropriate dilutions of DMSO.

SH-SY5Y, IMR-5 and IMR-32 human neuroblastoma cell lines were grown in DMEM medium from (Biowhittaker) plus 2mM L-glutamine from Eurobio (Courtaboeuf, France) or DMEM already supplemented with 2mM L-glutamine (Invitrogen, Barcelona, Spain), plus antibiotics and a 10% volume of FCS (Invitrogen, Cergy Pontoise, France or Barcelona, Spain). SH-SY5Y cell lines permanently transfected with pcDNA3/Bcl-2, pcDNA3/Bcl-XL and empty pcDNA3 vectors were grown like their untransfected counterparts. However, Geneticin (G-418) selection was maintained in the growing cultures before the terminal experiments (Ribas and Boix, 2004). In order to induce differentiation, SH-SY5Y cells were cultured on collagen coated plates and treated with 10 μM RA for five days.

HL-60 and Jurkat cells were grown in RPMI 1640 medium with 10% FCS and antibiotics from Invitrogen (Barcelona, Spain).

HCT116 human adenocarcinoma cell line was kindly provided by Dr. Vogelstein (The Howard Hughes Medical Institute, Sidney Kimmel Comprehensive Cancer Center, The Johns Hopkins School of Medicine, Baltimore, MD 21231, USA). HCT116 cells were cultured in McCoy's 5A (Biowhittaker) supplemented with antibiotics and 10% FCS. General culture conditions were an atmosphere of 5% CO_2 and a temperature of 37°C. Culture dishes and other plastic disposable tools were supplied by Corning (Corning, NY, USA). Indirubin treatments were performed on exponentially growing cultures at the indicated time and concentrations. Control experiments were carried also using appropriate dilutions of DMSO.

MDA-MB-231 cells (derived from hormone-independent breast cancer) were cultured in DMEM supplemented with 10% FCS. For experiments, these cells were seeded in 24-well boxes or in 35 mm Petri dishes at appropriate densities (4.10^4 cells per well for cell growth experiments; 10^5 cells per dish for cell cycle analysis) and exposed to indirubins as indicated.

Cell proliferation and cell cycle analysis

Propidium iodide (PI) staining was performed as follows. First, SH-SY5Y cells were harvested from the culture plates and washed once with PBS (Phosphate Buffered Saline,

pH 7.4). Second, 1-2x10^5 cells were incubated for 15 min in 25 μg/ml propidium iodide, 10 μg/ml RNase A, and 0.1% Triton X-100. Flow cytometry readings were obtained by an EPICS® XL unit from Coulter Científica, SA (Madrid, Spain). Data were processed by means of WinMDI (a free software from Joe Trotter) in order to obtain monoparametric DNA histograms. Finally, these histograms were analysed with the Multi-Cycle software.

Cell death and cell viability assessments

Cell death characterization based on nuclear morphology was assessed by double staining with 0.05 μg/ml bisBenzimide and 25 μg/ml propidium iodide. Cell viability was determined by means of the MTS method. Both procedures have been previously described in detail (Ribas and Boix, 2004). For evaluation of DNA laddering, cell DNA was extracted and electrophoresed in 1.5% agarose gels to evidence the internucleosomal fragmentation typical of apoptosis.

Caspase assay

The measurement of caspase activity is based on determining the fluorescence released from the AcDEVDafc synthetic substrate after its direct addition to the culture medium, detergent lysis, and incubation at 37º. This method is devised to be applied to 96 multiwell plates. It allows kinetic determinations of caspase activation and the characterization of multiple drugs simultaneously. (Ribas et al., 2005).

Electrophoresis and Western blotting

Whole cell extracts were obtained in buffer containing 100 mM Tris/HCl pH. 6.8, 1mM EDTA, 2% SDS. Following heat denaturation for 3 minutes, proteins were separated by 10 % SDS-PAGE (0.7 mm thick gels) ($p27^{Kip1}$) or by 10 % NuPAGE pre-cast Bis-Tris polyacrylamide mini gel electrophoresis system (Invitrogen) with MOPS SDS (p53, $p21^{Cip1}$, actin) or MES SDS (cytochrome C) running buffer depending on protein size. Proteins were transferred to 0.45 μm nitrocellulose filters (Schleicher and Schuell). These were blocked with 5 % low fat milk in Tris-Buffered Saline - Tween-20, incubated for 1 h with antibodies (anti-$p27^{KIP1}$: 1:1000; anti-actin: 1:1000; anti-Bcl-2, 1.2000; anti-Bcl-XL, 1:5000 ; anti-tubulin, 1:4000; anti-STAT3: 1:1000) or overnight at 4°C (anti-p53: 1:1000; $p21^{Cip1}$: 1:1000; cytochrome C: 1:1000; anti-actin: 1:5000 (STAT3 experiment);

anti-phosphoTyr705-STAT3: 1:1000) and analyzed by Enhanced Chemiluminescence (ECL, Amersham).

To study expression of p53 and $p21^{Cip1}$, cells were lysed for 30 minutes at 4°C in RIPA buffer (150 mM NaCl, 1% NP40, 0.5% deoxycholate, 0.1% SDS and 50 mM Tris-HCl pH 8.0) supplemented with a protease inhibitor cocktail (Roche). After centrifugation (12000g for 10 minutes), the protein concentration was determined in the supernatants by the Bradford protein assay (Bio-Rad). To study cytochrome C release from mitochondria, a 0.05% digitonin cytosolic extraction was performed (Ribas and Boix, 2004).

In the STAT3 study, cells were lyzed in 30 mM HEPES(pH 7.5), 10 mM NaCl, 5 mM $MgCl_2$, 25 mM NaF, 1 mM EGTA, 1 % Triton X-100, 10% glycerol, 2 mM sodium orthovanadate, 6.4 mg/mL p-nitrophenylphosphate and protease inhibitor cocktail (Roche). 73µg of total proteins was resolved on 10% NuPAGE with MOPS SDS running buffer.

ACKNOWLEDGMENTS

We are most thankful to our colleagues for providing reagents: Dr. Martin Goëttlicher, Dr. Steve Safe, Dr. Bert Vogelstein. This research was supported a grant from the EEC (FP6-2002-Life Sciences & Health, PRO-KINASE Research Project) (LM), and a "Cancéropole Grand-Ouest" grant (LM). KB was supported by a fellowship from the "Ministère de la Recherche". The Molecular Pharmacology Group wishes to thank the "Instituto de Salud Carlos III" (PI041488, 2005-2007) for financial support.

REFERENCES

Adachi J, Mori Y, Matsui S, Takigami H, Fujino J, Kitagawa H, Miller CA 3rd, Kato T, Saeki K and Matsuda T. (2001). *J. Biol. Chem.,* **276**, 31475-31478.

Bach S, Blondel M and Meijer L. (2006). In *Monographs on enzyme inhibitors. Volume 2. CDK inhibitors and their potential as anti-tumor agents* (E Yue and PJ Smith, editors). CRC Press, in press.

Baehecke EH. (2005). *Nat. Rev. Mol. Cell Biol.*, **6**, 505-510.

Balfour-Paul, J. (1998). *Indigo*. British Museum Press.

Benson C, Kaye S, Workman P, Garrett M, Walton M and de Bono J. (2005). *Br. J. Cancer*, **92**, 7-12.

Bertrand JA, Thieffine S, Vulpetti A, Cristiani C, Valsasina B, Knapp S, Kalisz HM, and Flocco M. (2003) *J. Mol. Biol.*, **33**, 393-407.

Broker LE, Kruyt FA and Giaccone G. (2005). *Clin. Cancer Res.*, **11**, 3155-3162.

Caserta TM, Smith AN, Gultice AD, Reedy MA and Brown TL. (2003). *Apoptosis*, **8**, 345-352.

Chipuk JE, and Green DR. (2005). *Nat. Rev. Mol. Cell Biol.*, **6**, 268-275.

Cohen P. (2002). *Nature Rev. Drug Discovery*, **1**, 309-315.

Cooksey CJ. (2001). *Molecules,* **6**, 736-769.

Damiens E, Baratte B, Marie D, Eisenbrand G and Meijer L. (2001). *Oncogene*, **20**, 3786-3797.

Davies TG, Tunnah P, Meijer L, Marko D, Eisenbrand G, Endicott JA and Noble MEM. (2001). *Structure*, **9**, 389-397.

Degterev A, Huang Z, Boyce M, Li Y, Jagtap P, Mizushima N, Cuny GD, Mitchison TJ, Moskowitz MA and Yuan J. (2005). *Nature Chem. Biol.*, **1**, 112-119.

Denison MS and Nagy SR. (2003). *Annu. Rev. Pharmacol. Toxicol.,* **43**, 309-334.

Elferink CJ. (2003). In "*Cell cycle regulators as therapeutic targets*". Meijer L, Jezequel A and Roberge M (ed). *Progr. Cell Cycle Res.*, **5**, 261-267.

Fischer PM. (2004). *Curr. Medicin. Chem.*, **11**, 1563-1583.

Fischer PM, Endicott J and Meijer L. (2003). In "*Cell Cycle Regulators as Therapeutic Targets*", L Meijer, A Jézéquel and M Roberge, Eds., *Progr. Cell Cycle Res.*, vol. 5, Editions "Life in Progress", Station Biologique de Roscoff, France, 235-248.

Fischer PM and Gianella-Borradori A. (2005) *Exp. Opin. Investig. Drugs*, **14**, 457-477.

Guengerich FP, Sorrells JL, Schmitt S, Krauser JA, Aryal P and Meijer L. (2004). *J. Med. Chem.*, **47**, 3236-3241.

Hoessel R, Leclerc S, Endicott J, Noble M, Lawrie A, Tunnah P, Leost, Damiens E, Marie D, Marko D, Niederberger E, Tang W, Eisenbrand G and Meijer L. (1999). *Nature Cell Biology*, **1**, 60-67.

Holton S, Merckx A, Burgess D, Doerig C, Noble M and Endicott J. (2003). *Structure*, **11**, 1329-1337.

Jaattela M. (2004). *Oncogene*, **23**, 2746-2756.

Jautelat R, Brumby T, Schafer M, Briem H, Eisenbrand G, Schwahn S, Kruger M, Lucking U, Prien O and Siemeister G. (2005). *Chembiochem.*, **6**, 531-540.

Kane DJ, Ord T, Anton R, Bredesen DE. (1995) *J. Neurosci. Res.* **40**, 269-275.

Kawanishi M, Sakamoto M, Ito A, Kishi K and Yagi T (2003). *Mutat. Res.*, **540**, 99-105.

Knockaert M, Blondel M, Bach S, Leost M, Elbi C, Hager G, Naggy SR, Han D, Denison M, Ffrench M, Ryan XP, Magiatis P, Polychronopoulos P, Greengard P, Skaltsounis L and Meijer L. (2004). *Oncogene,* **23,** 4400-4412.

Knockaert M, Greengard P and Meijer L. (2002). *Trends Pharmacol. Sci.*, **23**, 417-425.

Kolluri SK, Weiss C, Koff A and Göttlicher M. (1999). *Genes & Dev.,* **13**, 1742-1753.

Kosmopoulou MN, Leonidas DD, Chysina ED, Bischler N, Eisenbrand G, Sakarellos CE, Pauptit R and Oikonomakos NG. (2004). *Eur. J. Biochem.*, **271**, 2280-2290.

Leclerc S, Garnier M, Hoessel R, Marko D, Bibb JA, Snyder GL, Greengard P, Biernat J, Mandelkow E-M, Eisenbrand G and Meijer L. (2001). *J. Biol. Chem.,* **276**, 251-260.

Lee JW, Moon MJ, Min HY, Chung HJ, Park EJ, Park HJ, Hong JY, Kim YC and Lee SK. (2005). *Bioorg. Med. Chem. Lett.*, **15**, 3948-3952.

Lu H, Chang DJ, Baratte B, Meijer L and Schulze-Gahmen U. (2005). *J. Med. Chem*., **48**, 737-743.

Mapelli M, Massimiliano L, Crovace C, Seeliger M, Tsai LH, Meijer L and Musacchio A. (2005). *J. Med. Chem.*, **48**, 671-679.

Marko D, Schätzle S, Friedel A, Genzlinger A, Zankl H, Meijer L and Eisenbrand G. (2001). *British J. Cancer*, **84,** 283-289.

Meijer L, Borgne A, Mulner O, Chong JPJ, Blow JJ, Inagaki N, Inagaki M, Delcros JG and Moulinoux JP. (1997). *Eur. J. Biochem.*, **243**, 527-536.

Meijer L, Skaltsounis AL, Magiatis P, Polychronopoulos P, Knockaert M, Leost M, Ryan XP, Vonica CD, Brivanlou A, Dajani R, Tarricone A, Musacchio A, Roe, SM, Pearl L and Greengard P. (2003). *Chem. & Biol.*, **10**, 1255-1266.

Merz KH, Schwahn S, Hippe F, Muhlbeyer S, Jakobs S and Eisenbrand G. (2004). *Int. J. Clin. Pharmacol. Ther.*, **42**, 656-658.

Nam S, Buettner R, Turkson J, Kim D, Cheng JQ, Muehlbeyer S, Hippe F, Vatter S, Merz KH, Eisenbrand G and Jove R. (2005). *Proc. Natl. Acad. Sci. U.S.A.*, **102**, 5998-6003.

Noble ME, Endicott JA and Johnson LN. (2004). *Science*, **303**, 1800-1805.

Polychronopoulos P, Magiatis P, Skaltsounis L, Myrianthopoulos V, Mikros E, Tarricone A, Musacchio A, Roe SM, Pearl L, Leost M, Greengard P and Meijer L. (2004). *J. Med. Chem.*, **47**, 935-94.

Ribas J, Gomez-Arbones X, Boix J. (2005). *Eur. J. Pharmacol*., **524**, 49-52.

Ribas J, Boix J. (2004). *Exp. Cell Res*., **295**, 9-24.

Spink BC, Hussain MM, Katz BH, Eisele L and Spink DC. (2003). *Biochem. Pharmacol.*, **66**, 2313-2321.

Sugihara K, Kitamura S, Yamada T, Okayama T, Ohta S, Yamashita K, Yasuda M, Fujii-Kuriyama Y, Saeki K, Matsui S and Matsuda T. (2004). *Biochem. Biophys. Res. Commun*., **318**, 571-578.

Teng X, Degterev A, Jagtap P, Xing X, Choi S, Denu R, Yuan J and Cuny GD. (2005). *Bioorg. Med. Chem. Lett.*, 2005 Sep 6, in press

Vermeulen K, Van Bockstaele DR and Berneman ZN. (2003). *Cell Prolif.*, **36**, 131-149.

Weinmann H and Metternich R. (2005). *ChemBioChem*., **6**, 455-459.

Weiss C, Kolluri SK, Kiefer F and Göttlicher M. (1996). *Exp. Cell Res.,* **226**, 154-163.

Wu ZL, Aryal P, Lozach O, Meijer L and Guengerich FP. (2005). *Chem. & Biodiv.*, **2**, 51-65.

Xiao Z, Hao Y, Liu B and Qian L (2002). *Leuk. Lymphoma,* **43**, 1763-1768.

Yuste VJ, Sanchez-Lopez I, Sole C, Encinas M, Bayascas JR, Boix J and Comella JX. (2002) *J. Neurochem.* **80**, 126-139.

TABLES

Table 1. Effects of various bromo- substituted indirubins and various 7-halogeno-substituted indirubins on three protein kinases. A series of indirubin analogues were tested at various concentrations in the kinase assays, as described in the Material and Methods section. IC_{50} values were calculated from the dose-response curves and are reported in μM.

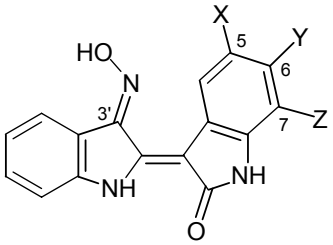

	X	Y	Z	
1	H	H	H	(**IO**)
2	Br	H	H	(**5BIO**)
3	H	Br	H	(**6BIO**)
4	H	H	Br	(**7BIO**)
5	H	H	Cl	(**7ClO**)
6	H	H	I	(**7IIO**)
7	H	H	F	(**7FIO**)

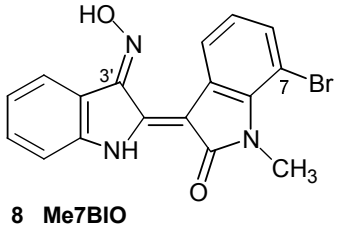

8 Me7BIO

N°	Compound	GSK-3 α/β	CDK1/ cyclin B	CDK5/ p25
1	indirubin-3'-oxime (**IO**)	0.022	0.180	0.100
2	5-bromoindirubin-3'-oxime (**5BIO**)	0.016	0.045	0.028
3	6-bromoindirubin-3'-oxime (**6BIO**)	0.005	0.320	0.083
4	7-bromoindirubin-3'-oxime (**7BIO**)	32	22	33
5	7-chloroindirubin-3'-oxime (**7ClO**)	21	3.7	6
6	7-iodoindirubin-3'-oxime (**7IIO**)	16	66	77
7	7-fluoroindirubin-3'-oxime (**7FIO**)	0.270	1.5	0.510
8	1-methyl-7-bromoindirubin-3'-oxime (**Me7BIO**)	> 100	> 100	> 100

Table 2. ProQinase selectivity profile of IO, 5BIO, 6BIO and 7BIO. The four indirubins were tested at various concentrations in 85 kinase assays, as described in the Material and Methods section. *n.t.*, not tested. IC_{50} values, calculated from the dose-response curves, are reported in μM and underlined according to a gray scale code:

IC_{50} value (μM)	< 0.1	0.1 - 1	1 - 10	10 - 100	> 100

KINASE	IO	5BIO	6BIO	7BIO
ABL1	>100	>100	3.4	>100
AKT1	>100	>100	>100	>100
AKT2	>100	>100	>100	>100
AKT3	n.t.	n.t.	>100	>100
Aurora-A	0.20	0.23	0.43	55
Aurora-B	1.4	35	1.5	4.7
Aurora-C	0.57	34	2.3	6.6
BRK	17	>100	4.6	33
CDK1/CycB	20	2.1	21	>100
CDK2/CycA	2.3	0.46	0.71	>100
CDK2/CycE	2.2	0.12	0.12	>100
CDK3/CycE	0.15	0.04	0.07	>100
CDK4/CycD1	0.56	1.33	0.80	>100
CDK6/CycD1	0.19	0.05	0.17	>100
CHK1	35	>100	12	>100
CK2	>100	>100	>100	>100
COT	*n.t.*	*n.t.*	75	49
CSK	>100	>100	*n.t.*	*n.t.*
DAPK1	>100	>100	*n.t.*	*n.t.*
EGF-R	102	>100	9.1	27
EPHA1	53	>100	38	44
EPHB1	56	>100	*n.t.*	*n.t.*
EPHB2	6.1	>100	5.0	33
EPHB3	>100	>100	34	28
EPHB4	8.6	>100	3.5	10.0
ERBB2	>100	>100	>100	26
ERBB4	>100	>100	>100	>100
FAK	0.99	>100	12	78
FGF-R1	0.74	0.83	0.43	36
FGF-R3	0.38	0.85	0.42	23
FGF-R4	13	65	1.2	17
FGR	1.6	>100	0.09	20
FLT3	0.07	0.02	0.20	0.34
GSK3-beta	2.5	0.07	0.21	>100
IGF1-R	5.3	5.6	79	26
IKK-beta	>100	>100	>100	>100
INS-R	6.6	4.3	>100	>100
IRAK4	1.8	44	4.8	82
JAK2	33	>100	>100	>100
JNK3	25	>100	*n.t.*	*n.t.*
KIT	4.3	16	0.76	58
LCK	41	>100	3.1	>100
MET	>100	>100	>100	>100

KINASE	IO	5BIO	6BIO	7BIO
MST4	73	>100	*n.t.*	*n.t.*
MUSK	0.21	31	0.50	>100
NEK2	>100	>100	>100	>100
NEK6	>100	>100	>100	>100
NLK	>100	>100	>100	>100
PAK1	13	11	*n.t.*	*n.t.*
PAK2	>100	>100	*n.t.*	*n.t.*
PAK4	>100	91	*n.t.*	*n.t.*
PBK	>100	>100	>100	>100
PCTAIRE1	>100	>100	>100	>100
PCTAIRE2	*n.t.*	*n.t.*	15	>100
PDGFR-alpha	4.0	9.5	0.52	47
PDGFR-beta	3.4	3.4	0.88	>100
PIM1	>100	>100	91	>100
PIM2	*n.t.*	*n.t.*	>100	>100
PKC-alpha	>100	>100	>100	>100
PKC-beta1	>100	>100	>100	>100
PKC-beta2	>100	>100	>100	>100
PKC-delta	>100	>100	>100	65
PKC-epsilon	>100	>100	>100	>100
PKC-eta	>100	>100	>100	>100
PKC-gamma	>100	>100	>100	>100
PKC-iota	>100	>100	>100	>100
PKC-mu	>100	>100	>100	>100
PKC-theta	>100	>100	86	>100
PKC-zeta	>100	>100	>100	96
PLK1	>100	>100	>100	>100
PRK1	>100	>100	70	>100
RET	0.18	2.2	0.05	22
S6K	82	>100	6.1	>100
SGK1	0.14	1.6	*n.t.*	*n.t.*
SGK3	38	>100	5.8	>100
SNK	>100	>100	>100	>100
SRC	1.5	17	0.13	27
SYK	3.0	>100	6.2	85
TIE2	11	68	13	27
TSF1	0.87	13	2.9	3.3
TSK2	>100	>100	>100	>100
VEGF-R1	1.6	1.6	3.2	>100
VEGF-R2	0.19	0.25	0.56	23
VEGF-R3	0.09	0.08	0.22	11
WEE1	*n.t.*	*n.t.*	>100	>100

FIGURE LEGENDS

Figure 1. Effects of IO, 5BIO, 6BIO and 7BIO on the survival of SH-SY5Y cells. (**A**) SH-SY5Y cells were exposed for 24 h to increasing concentrations of **IO**, **5BIO**, **6BIO** or **7BIO**. Cell survival was estimated by the MTS reduction assay and is expressed in % of survival in untreated cells. Average ± s.e. of at least four independent experiments with three independent measurements per experiment. (**B**) A similar experience was performed but LDH release was assayed 24 hr after the addition of the indirubins. Average ± s.e. of two independent experiments with three independent measurements per experiment.

Figure 2. Effects of various 7-halogeno-indirubin-3'oxime (A) and 1-methyl-7-bromo-indirubin-3'oxime (B) on the survival of SH-SY5Y cells. SH-SY5Y cells were exposed for 48 h to increasing concentrations of 7-chloro-, 7-iodo-, 7-bromo-, or 7-fluoro-indirubin-3'oximes (**7CIO**, **7IIO**, **7BIO**, **7FIO,** respectively) (**A**) or 1-methyl-7-bromo-indirubin-3'oxime (**Me7BIO**) or **7BIO** (**B**). Cell survival was estimated by the MTS reduction assay and is expressed in % of survival in untreated cells. Average ± s.e. of three determinations.

Figure 3. Effects of 7BIO on cell proliferation and cell cycle distribution in MDA-MB-231 cells. (**A**) Cells were exposed at time 0 to various concentrations of **7BIO** and cell numbers were determined at various times. At 48 h, the culture medium was replaced by fresh medium devoid of **7BIO**. (**B**) Cells were exposed to various concentrations of **7BIO** for 24 h and their distribution in the various cell cycle phases was determined by FACS analysis.

Figure 4. The cytotoxic effect of 7BIO is independent of AhR. (**A**) Hepatocyte AhR-/- (BP8) and AhR+/+ (5L) cells were treated with 0.1 μM TCDD, or 10 μM **7BIO** or **Me7BIO** for 24 h or with the vehicle DMSO. The expression level of $p27^{KIP1}$ was determined by Western blotting using a specific antibody. Actin Western blotting was used as a loading control. (**B**) Both 7BIO and Me7BIO induce an Ah-dependent

accumulation in G0/G1. 5L and BP8 cells were cultured in the absence (control) or presence of DMSO or 10 μM **7BIO** or **Me7BIO** for 24 h, and the cell cycle phase distribution was determined by FACS analysis. (**C**) Both 5L and BP8 cell lines were exposed for 24 h to increasing concentrations of **7BIO** or **Me7BIO**. Cell survival was estimated by the MTT reduction assay and is expressed in % of survival in untreated cells. Average ± s.e. of three determinations.

Figure 5. 7BIO does not induce nor require p53 nor $p21^{CIP1}$ expression. (A) SH-SY5Y cells were treated with 12.5 μM **IO**, **5BIO**, **6BIO**, **7BIO** or **Me7BIO**, 1 μM staurosporine or 12.5 μM etoposide for 12 h. Cells were then harvested and proteins were resolved by SDS-PAGE followed by Western blotting using antibodies directed against p53, $p21^{CIP1}$ or actin (used as internal loading marker). (B-D) SH-SY5Y cells were treated with 12.5 μM **5BIO** or **7BIO** or 12.5 μM etoposide for various times. Cells were then harvested and proteins were resolved by SDS-PAGE followed by Western blotting using antibodies directed against p53 (B), $p21^{CIP1}$ (C) or actin (D). (E) wild-type (●) and p53-deprived (○) HCT-116 cells were exposed for 24 h to increasing concentrations of **7BIO** or **Me7BIO**. Cell survival was estimated by the MTS reduction assay and is expressed in % of survival in untreated cells. Average ± s.e. of three determinations.

Figure 6. 7BIO effects do not involve down-regulation of STAT3 tyrosine phosphorylation. MDA-MB-231 cells were either untreated or treated with 25 μM **IO**, **5BIO**, **6BIO**, **7BIO**, or the DMSO carrier for 4 h, or with 100 ng/ml of IFN-α for 5 min. Cellular proteins were resolved by SDS-PAGE followed by Western blotting using antibodies directed total STAT3 and Tyrosine-phosphorylated STAT3. Western blotting with anti-actin antibodies provided a loading marker.

Figure 7. 7BIO induces cell death much faster than other indirubins. SH-SY5Y cells were treated with 25 μM **IO**, **5BIO**, **6BIO**, **7BIO** or **Me7BIO** for 6, 12, 24, 36 or 48 h. Cell survival was assessed by the MTS procedure. Every point is the mean ± s.e. of two independent experiments with at least three independent measurements per experiment.

Figure 8. In contrast to IO, 5BIO and 6BIO, 7BIO induces non-apoptotic cell death in SH-SY5Y cells. SH-SY5Y cells were exposed for 24 h to 0.1 % DMSO (control) (**A**), 25 μM **IO** (**B**), 25 μM **5BIO** (**C**), 10 μM **6BIO** (**D**), 10 μM **7BIO** (**E**) or 10 μM **Me7BIO** (**F**). Following double staining of DNA with BisBenzimide and propidium iodide, cells were examined by fluorescence microscopy. Thick arrows: apoptosis (nuclear fragmentation); thin arrows: secondary necrosis; arrow heads: pycnotic nuclei. Scale bar: 20 μm.

Figure 9. 7BIO does not induce caspase activation. (A) SH-SY5Y cells were treated with **IO**, **5BIO**, **6BIO**, **7BIO** or **Me7BIO** for 24 h in the range of concentrations shown. The value of control untreated cells is placed at time 0. DEVDase activity was measured as arbitrary fluorescence units. Every point is the mean ± s.e. of at least three independent determinations. (B).The time course of effector caspase activity was determined in SH-SY5Y cells treated with 25μM **IO**, **5BIO**, **6BIO**, **7BIO** or **Me7BIO** for 24 h. Every point is the mean ± s.e. of at least three independent determinations.

Figure 10. 7BIO-induced cell death is not prevented by Q-VD-OPh, a general caspase inhibitor. (A) SH-SY5Y cells were treated with 25 μM **IO**, **5BIO**, **6BIO**, **7BIO** or **Me7BIO** for 48 h in the presence (black bars) or absence (white bars) of 10 μM Q-VD-OPh, a broad spectrum inhibitor of caspases. Cell survival was assessed by the MTS assay. Every point is the mean ± s.e. of four independent experiments with three independent measurements per experiment. In the control Q-VD-OPh graph only two independent experiments were performed. (B) Time-course of **7BIO**-induced cell death in the absence (○) or presence (●) of 10 μM Q-VD-OPh. Cells were exposed to 25 μM **BIO** at time 0 and cell survival was estimated at different time-points by the MTS assay. Each point is the mean ± s.e. of at least three independent experiments with three independent measurements per experiment.

Figure 11. IO, 5BIO and 6BIO, but not 7BIO, induce cytochrome C release and DNA laddering. (A) SH-SY5Y cells were treated with 12.5 μM **IO**, **5BIO**, **6BIO**, **7BIO** or **Me7BIO**, 0.25 μM staurosporine or 12.5 μM etoposide for 10 h. Cells were then

harvested and fractionated into a nuclear pellet and a cytoplasmic supernatant. The latter was resolved by SDS-PAGE followed by Western blotting using an anti-cytochrome C antibody. The antibody cross-reacts with an irrelevant protein used as an internal loading marker. (B) SH-SY5Y cells were treated with DMSO (0.25 %), 25 μM **IO**, **5BIO**, **6BIO**, **7BIO** or **Me7BIO**, or 25 μM (R)-roscovitine for 24 h. Cells were then harvested and internucleosomal DNA fragmentation was analyzed by electrophoresis in 1.5 % agarose gels.

Figure 12. In contrast to STS-induced apoptosis 7BIO-induced cell death is resistant to the protective effects of cell differentiation (A) or Bcl-2 / Bcl-XL overexpression (B, C). (A) SH-SY5Y cells were either treated with RA during 5 days to induce quiescence and differentiation (white bars) or kept proliferating (black bars). After 24 h of treatment with STS (1 μM), **7BIO** (25 μM) or racemic Roscovitine (50 μM), cell viability was determined by the MTS procedure. Bar value is the mean ± s.e. of at least 6 independent determinations. (B) SH-SY5Y cells, permanently transfected with the vectors pcDNA3/Bcl-XL (●), pcDNA3/Bcl-2 (○) and empty pcDNA3 (■), were treated with either STS (2 μM) or **7BIO** (25 μM). Cell viability was analyzed by the MTS procedure at 9 and 24 h of treatment. In the time course plots, every point is the mean ± s.e. of three independent experiments with six independent values per experiment. (C) The Bcl-XL and Bcl-2 content of pcDNA3/Bcl-2 (1), pcDNA3/Bcl-XL (2) and pcDNA3/empty (3) transfected SH-SY5Y cells was assessed during the viability determination experiments by Western blotting. Tubulin content was used to control for protein load.

Figure 13. 7BIO induces caspase-independent cell death in four additional cell lines. IMR-5, IMR-32, HL-60 and Jurkat cells were challenged with increasing concentrations of **7BIO** for 24 h and cell viability was determined by the MTS procedure (left). Every point is the mean ± s.e. of three independent experiments with six independent measurements per experiment. The same cell lines were subjected for 24 h to treatments with STS (1μM), **5BIO** (25 μM), **7BIO** (25 μM) or left untreated (U) and the activation

of effector caspases (DEVDase activity in arbitrary fluorescent units) was measured (right). Bar value is the mean ± s.e. of 6 independent determinations.

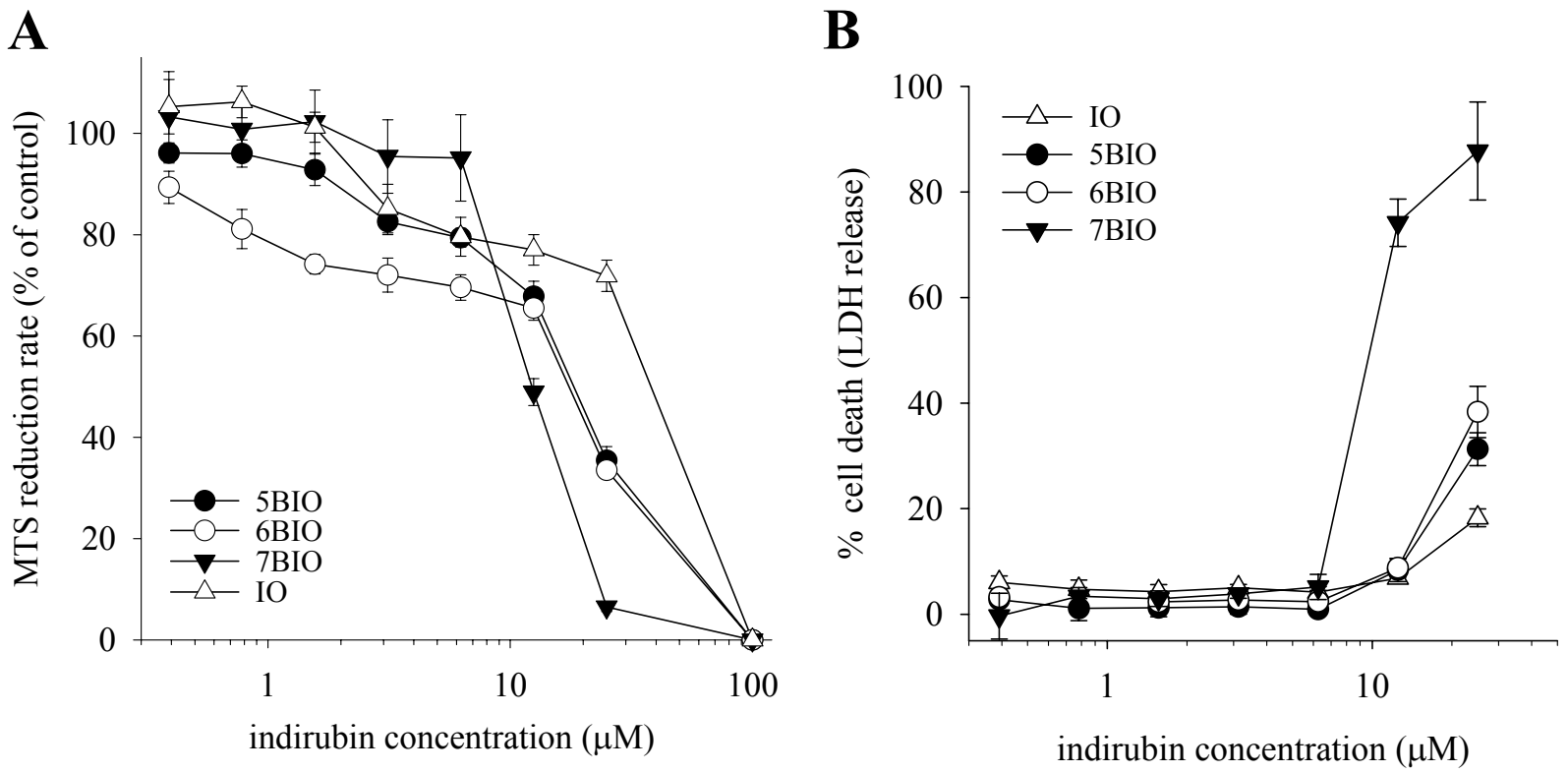

Ribas et al.
Figure 1

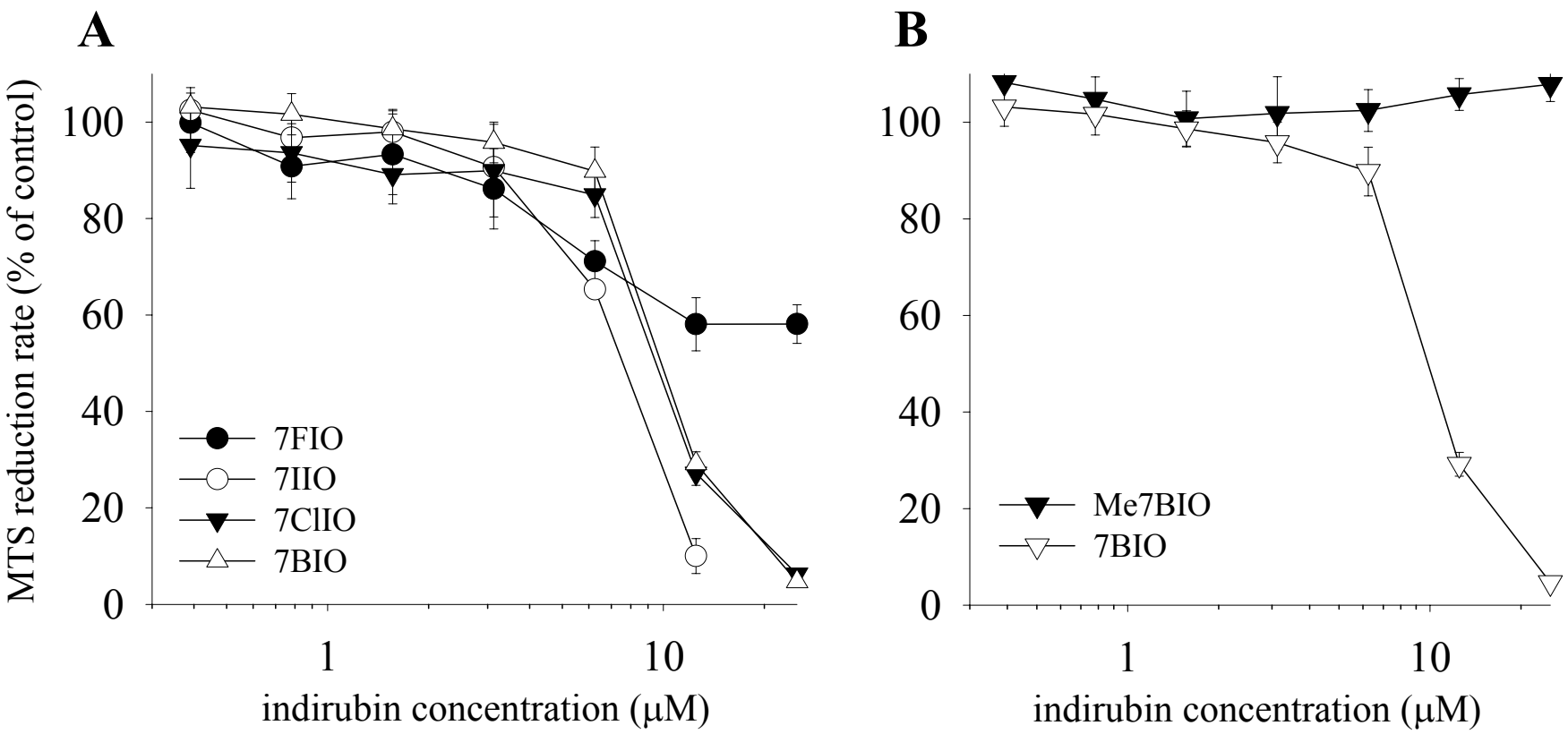

Ribas et al.
Figure 2

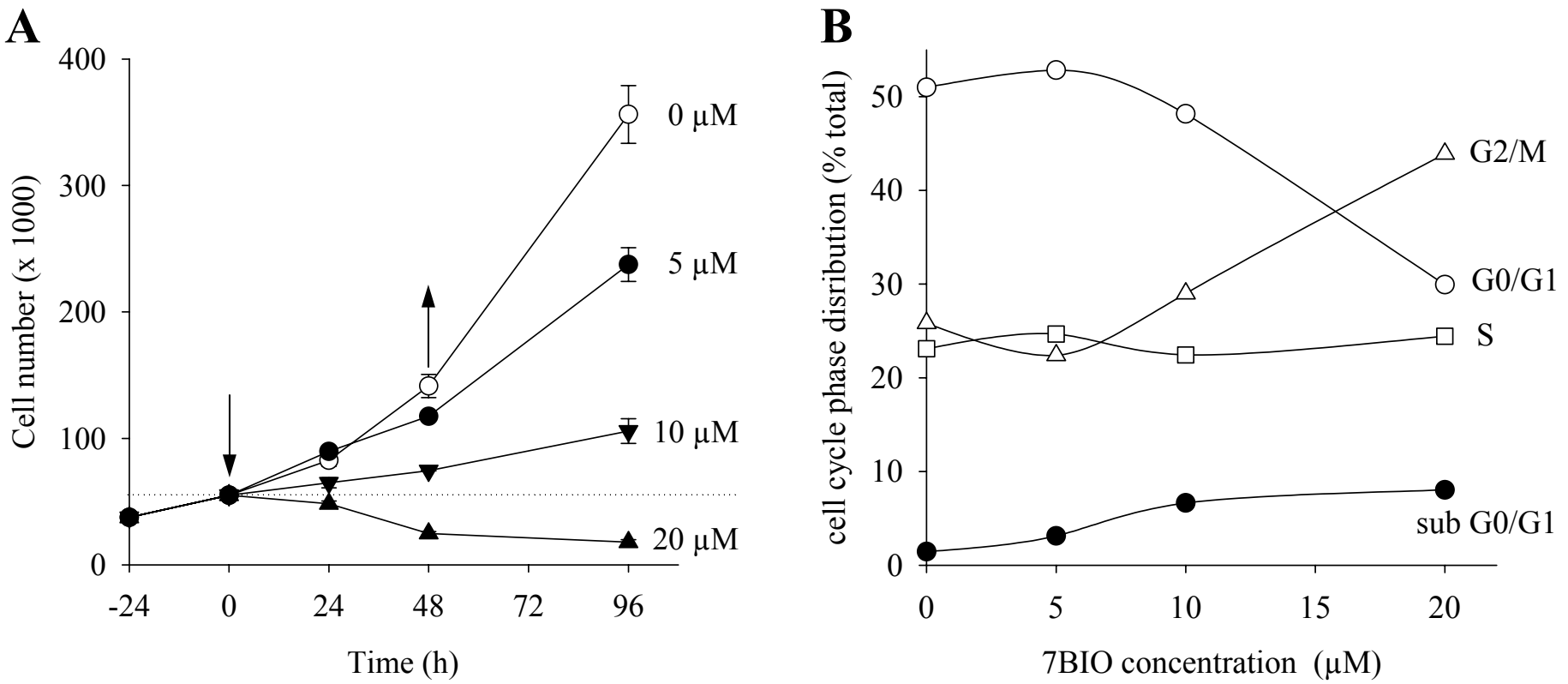

Ribas et al.
Figure 3

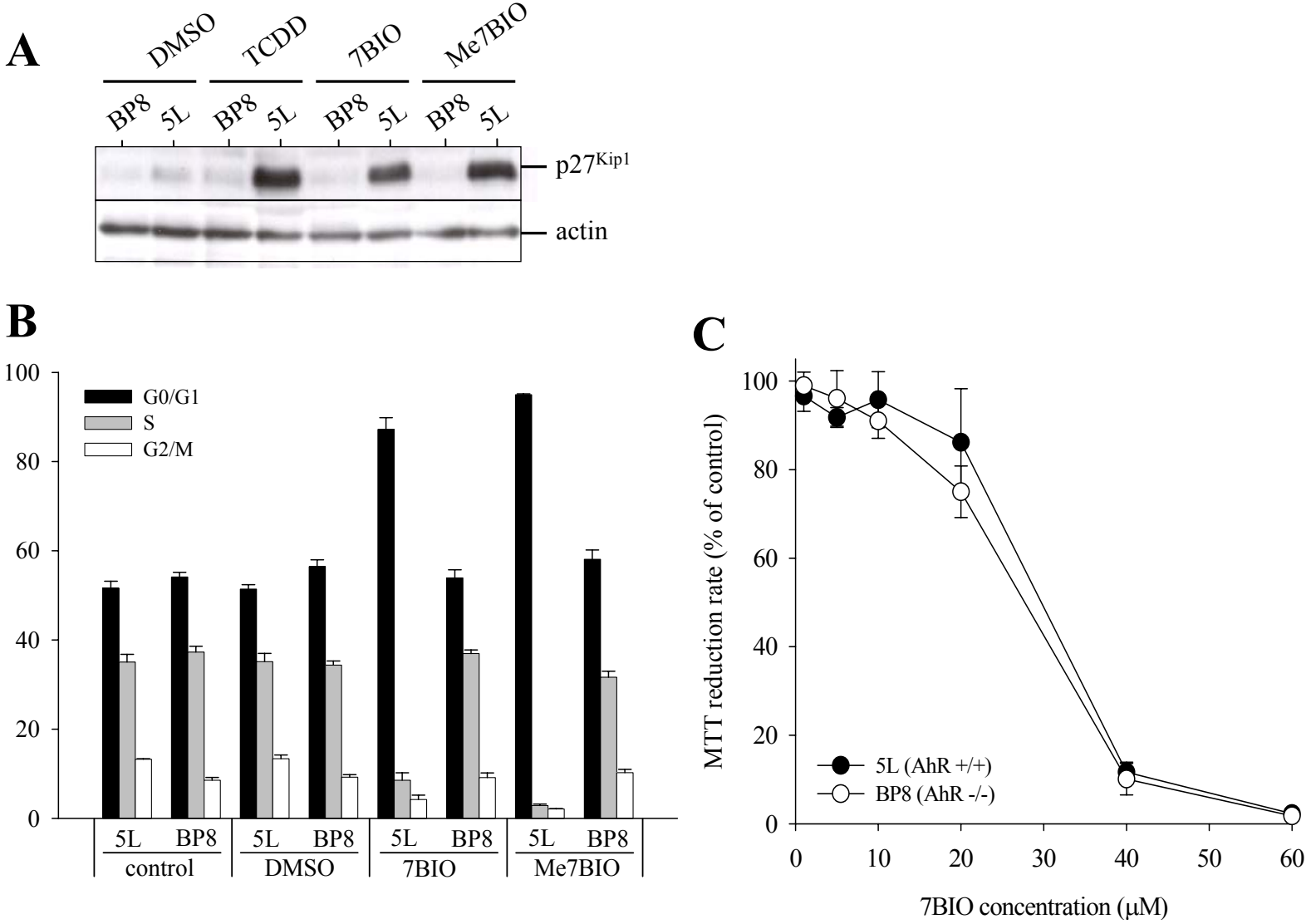

Ribas et al.
Figure 4

A

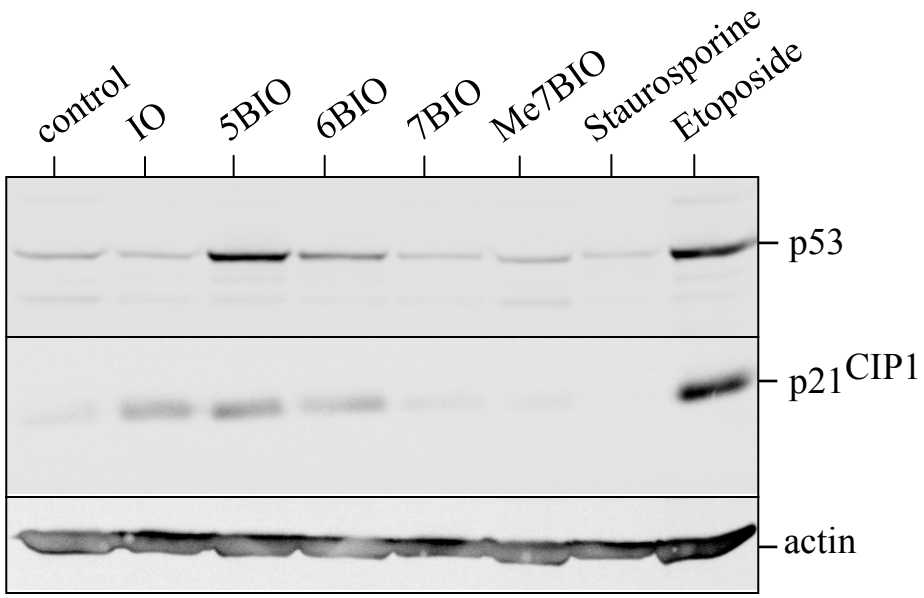

Ribas et al.
Figure 5A

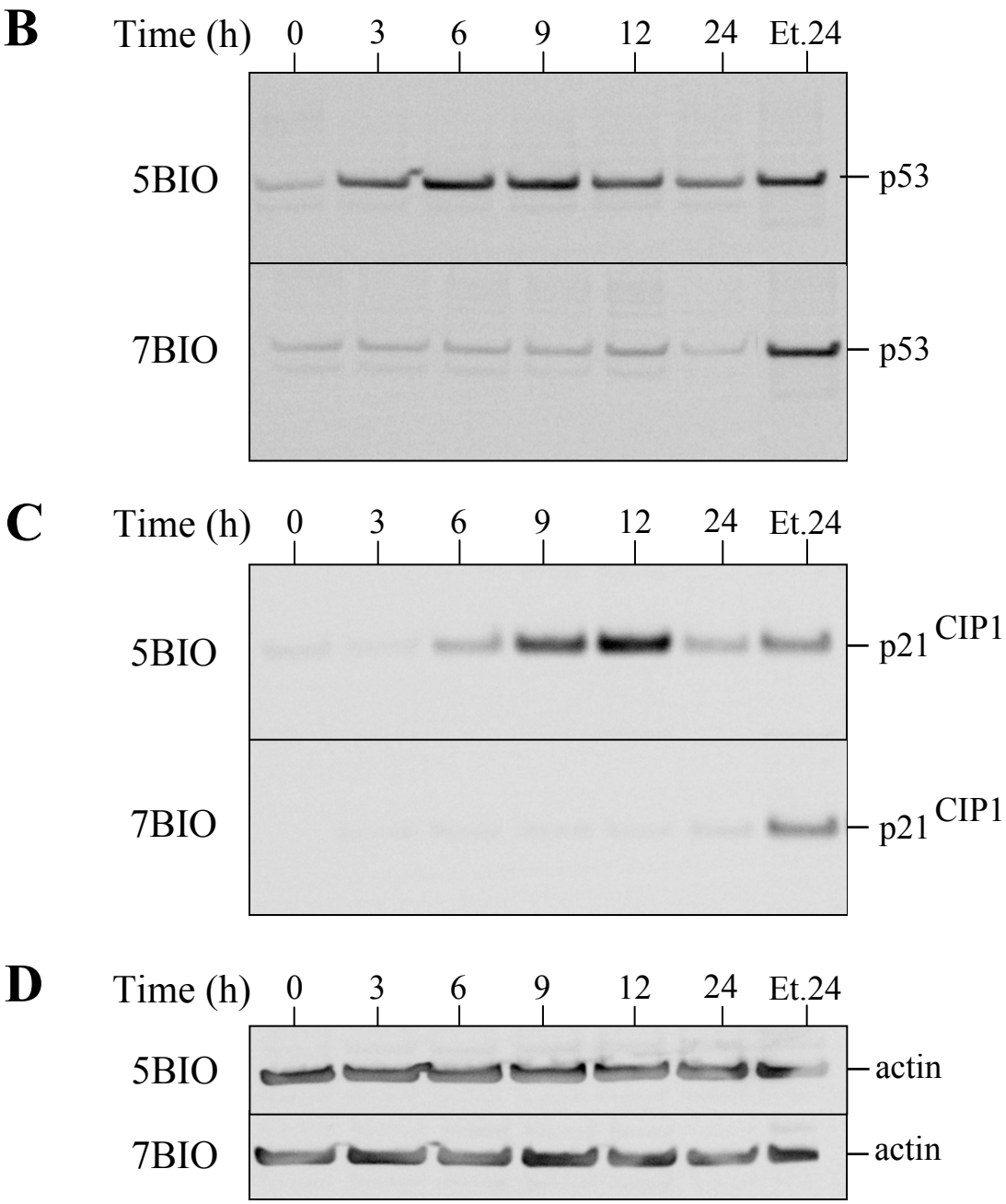

Ribas et al.
Figure 5B-D

E

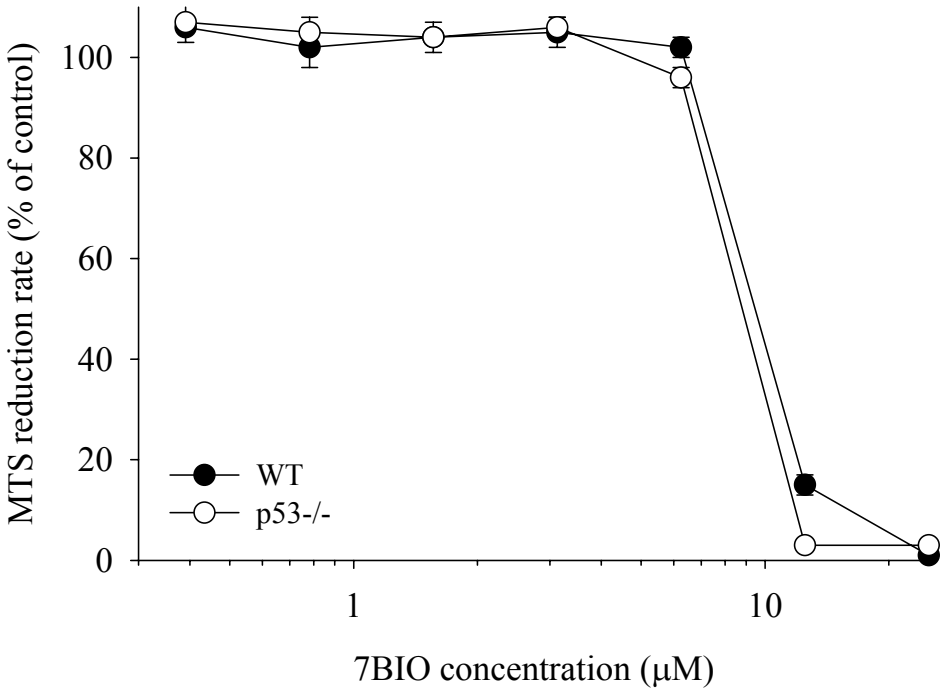

Ribas et al.
Figure 5E

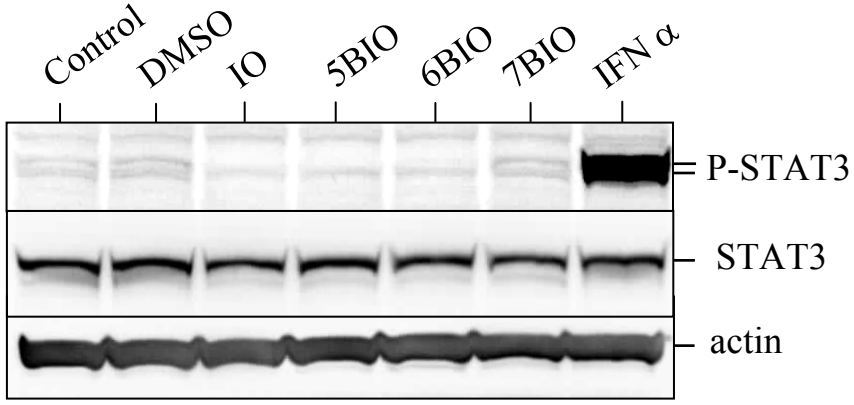

Ribas et al.
Figure 6

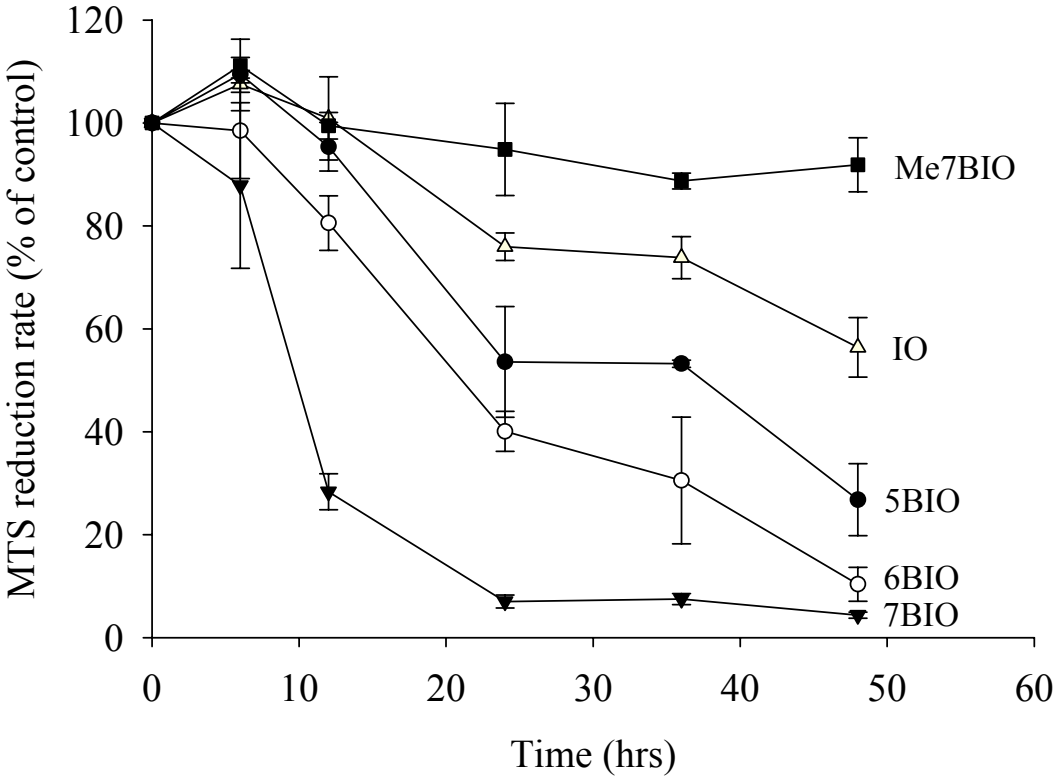

Ribas et al.
Figure 7

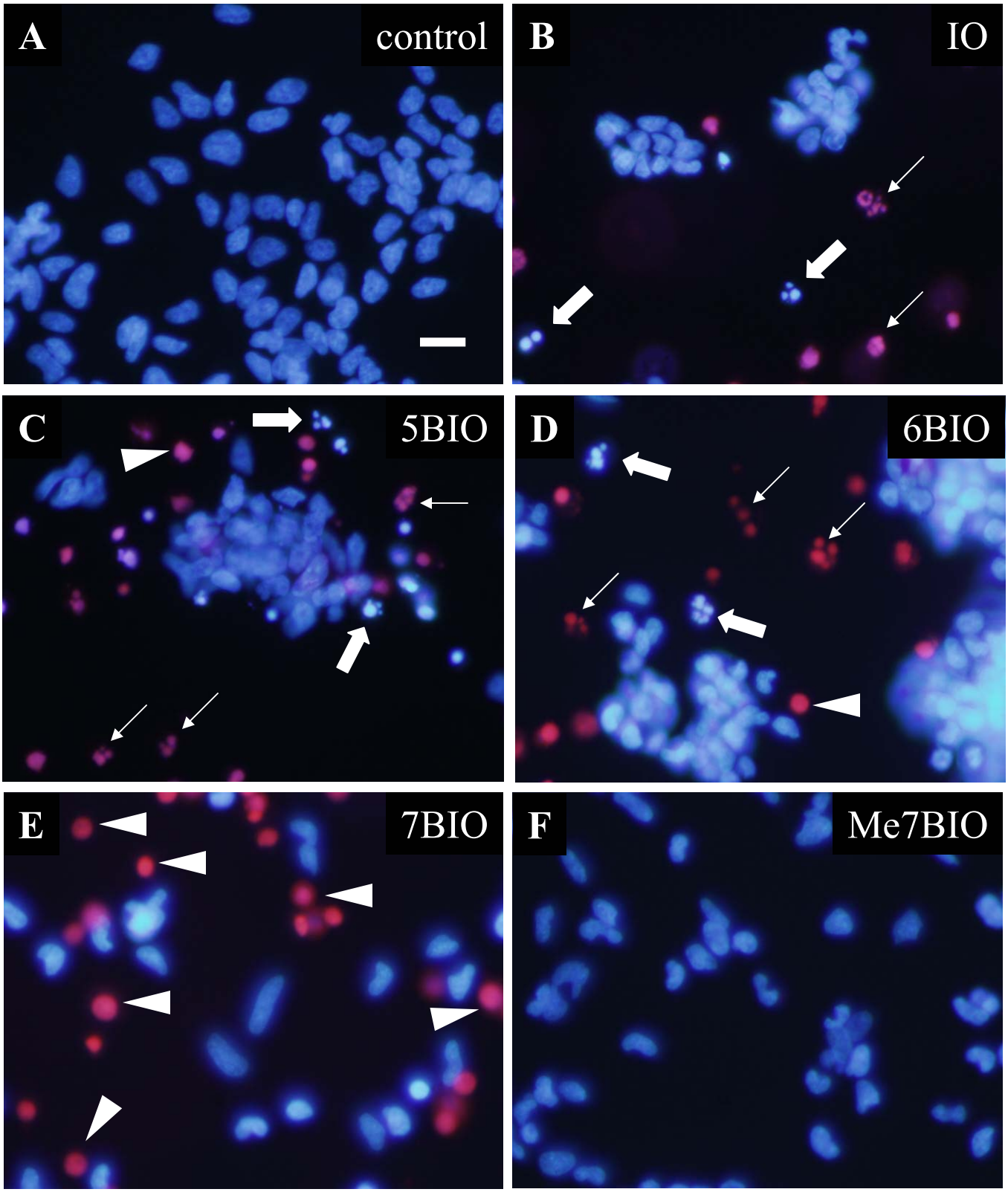

Ribas et al.
Figure 8

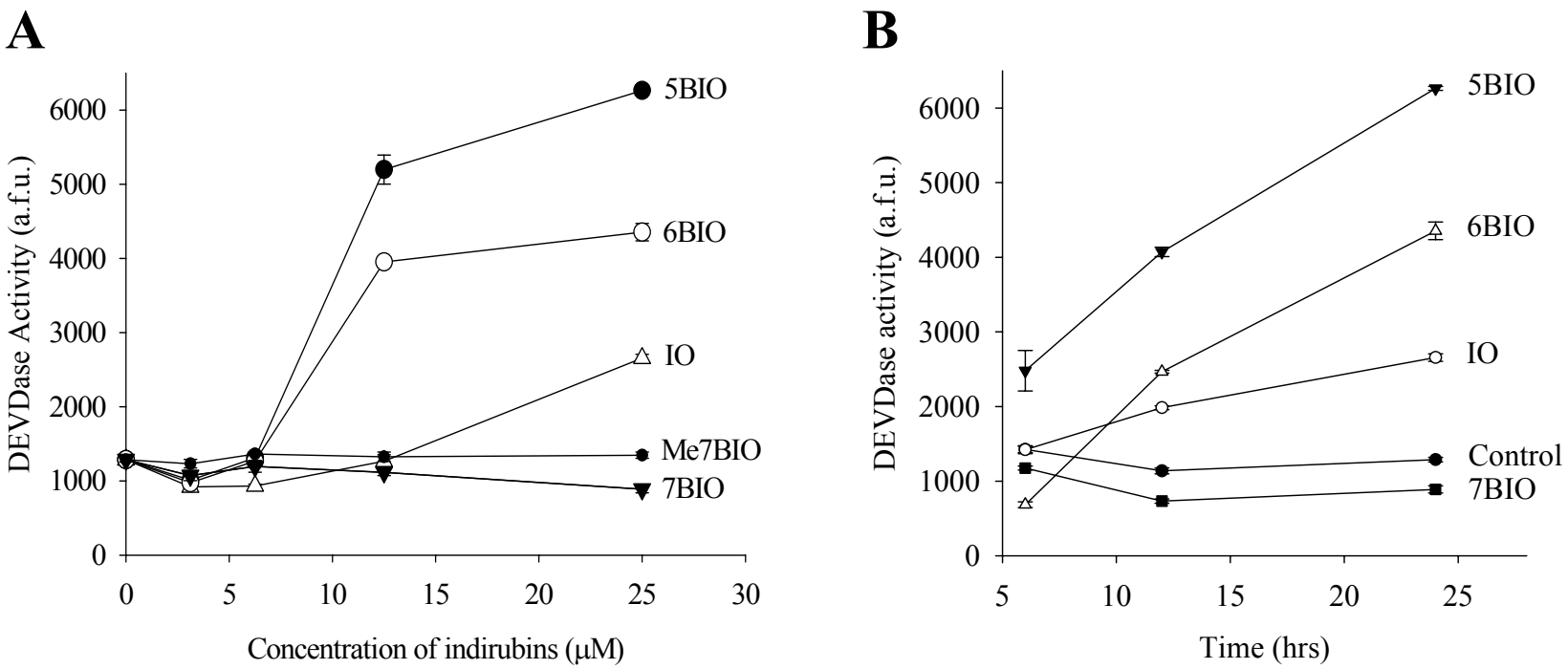

Ribas et al.
Figure 9

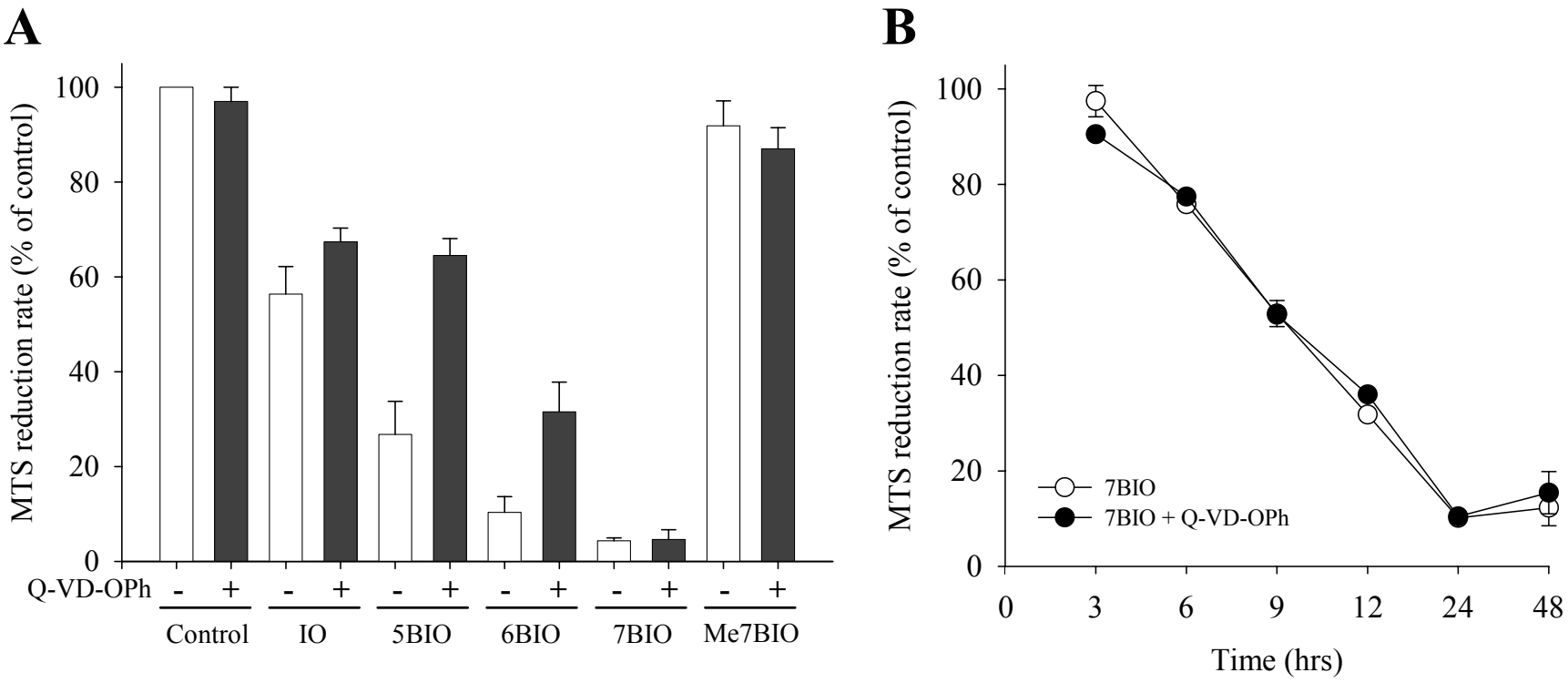

Ribas et al.
Figure 10

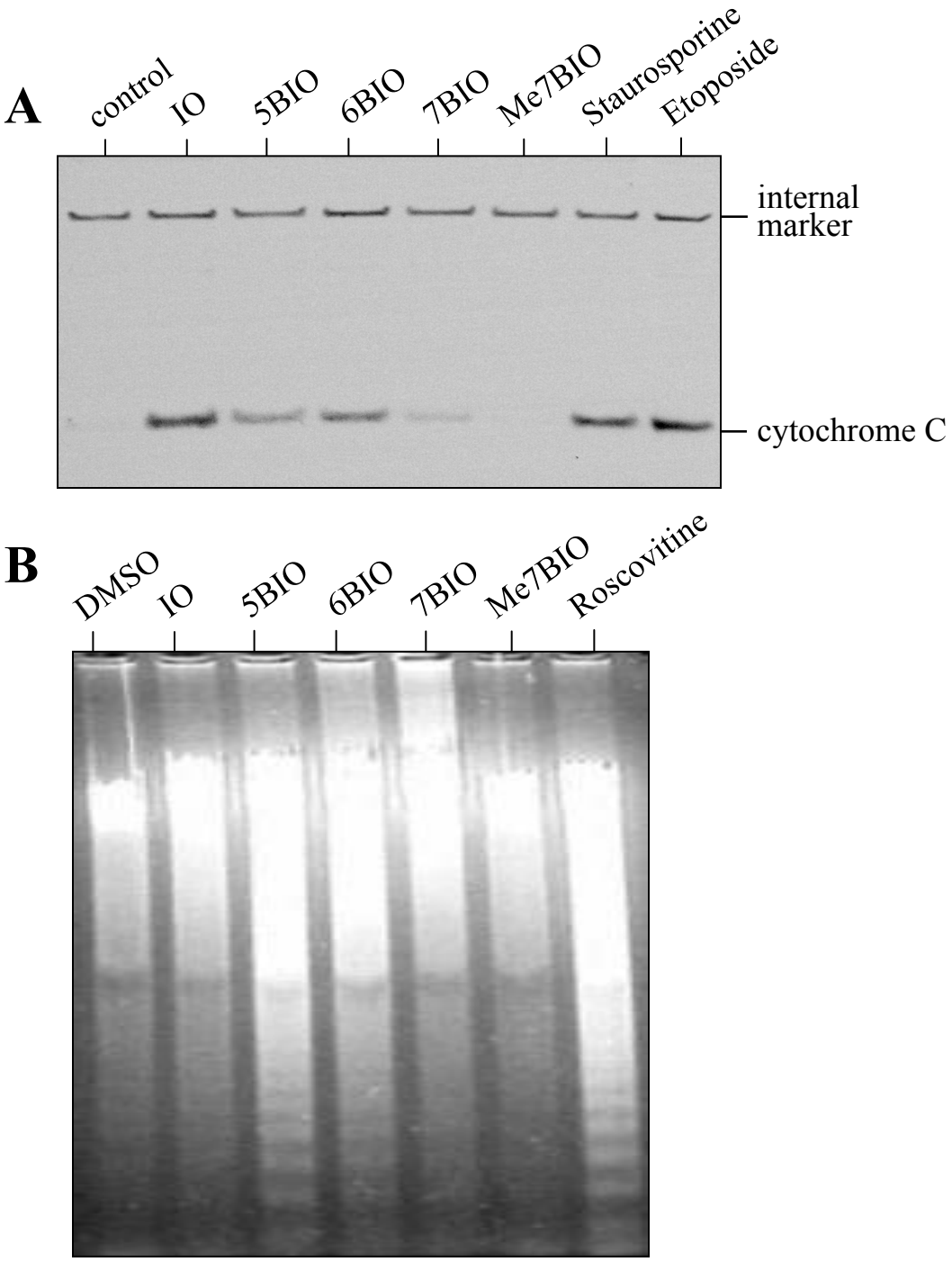

Ribas et al.
Figure 11

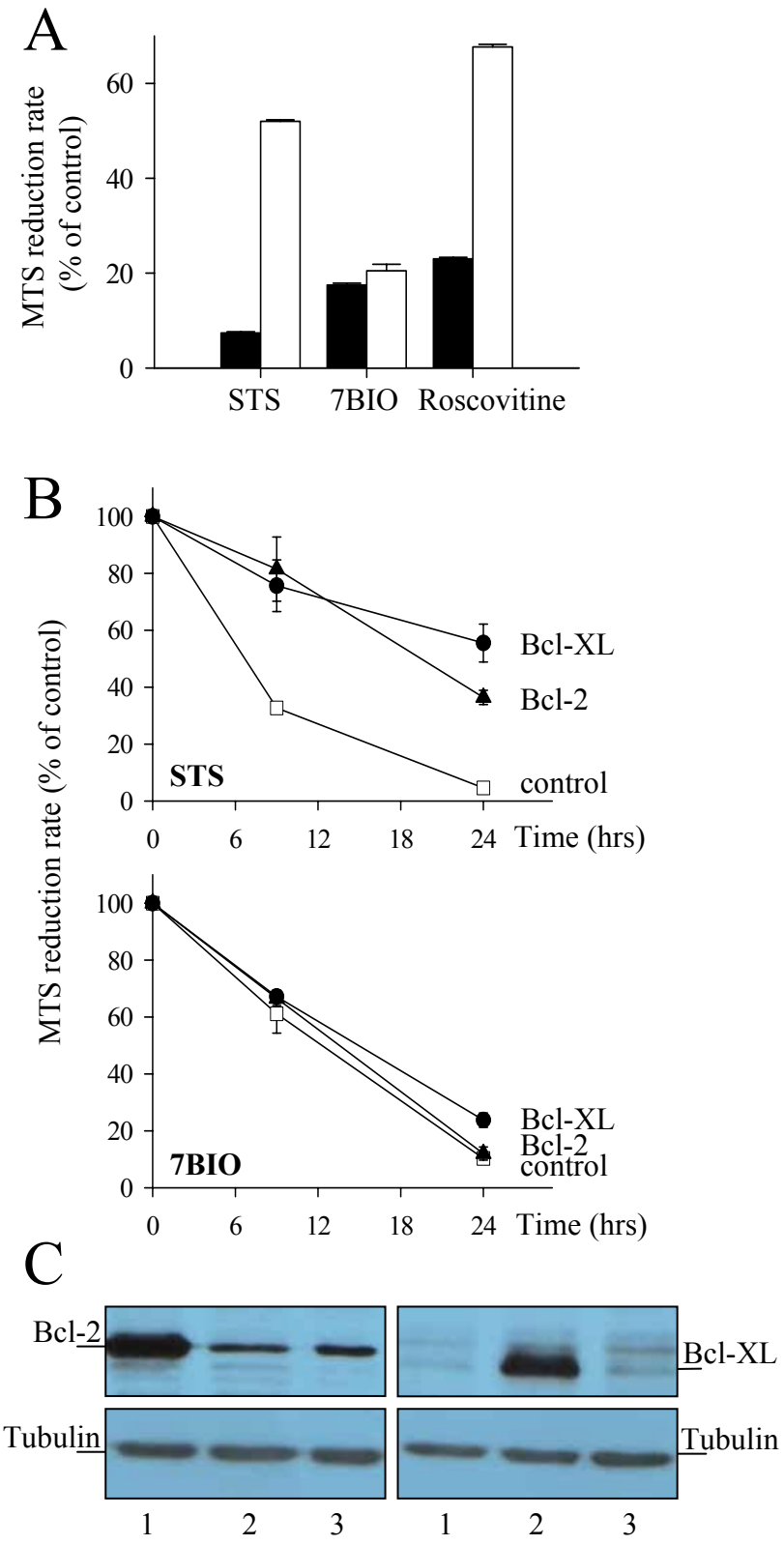

Ribas et al.
Figure 12

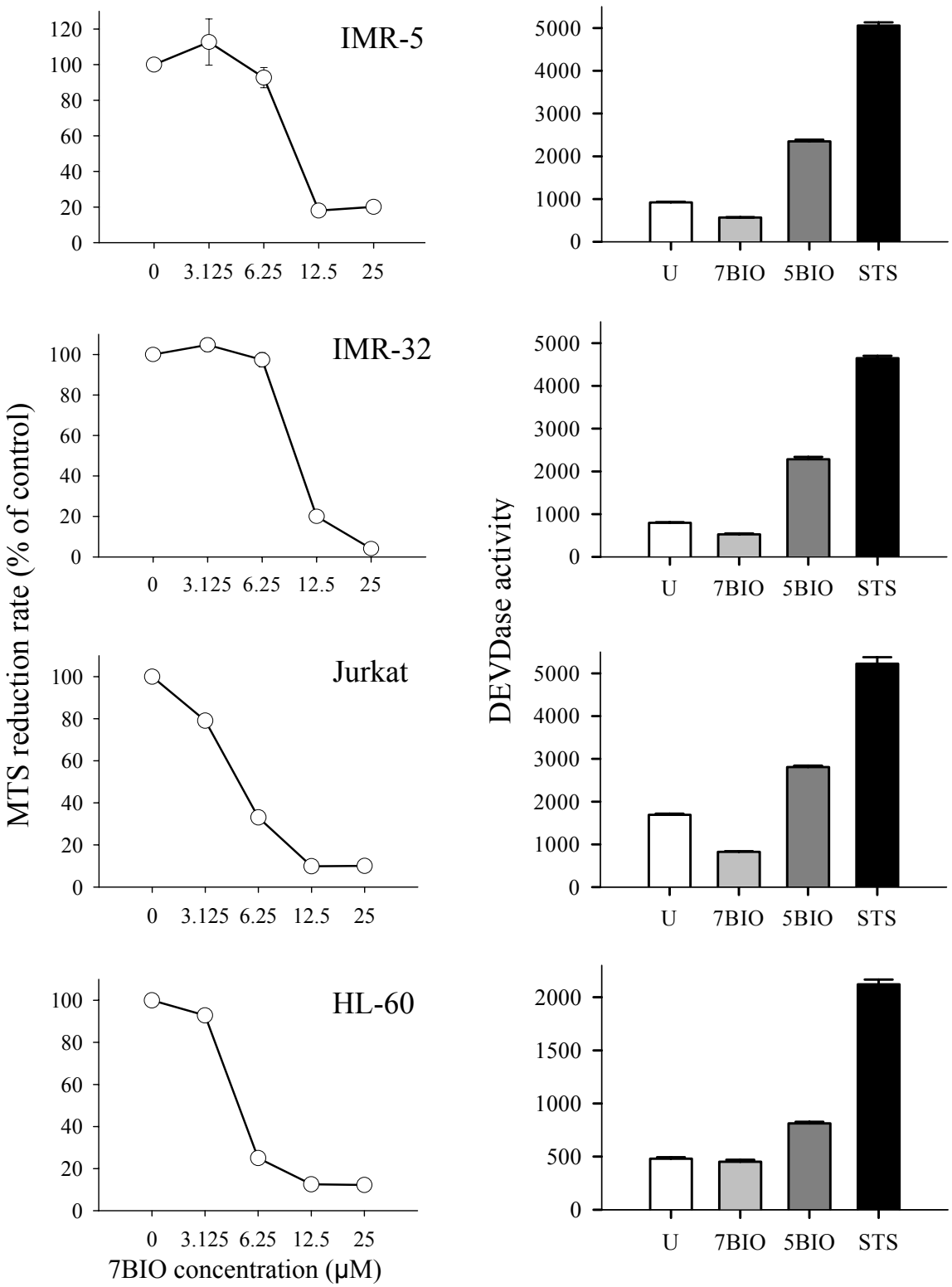

Ribas et al.
Figure 13